

University of Southern Queensland
Faculty of Engineering and Surveying

The use of low-cost photogrammetry techniques to create an
accurate model of a human skull.

A dissertation submitted by:

Heidi Jane Belbin

W0109098

In fulfilment of the requirements of:
Bachelor of Spatial Science (Honours)
(Major: Surveying)

2015

Abstract

There has been increasing interest in low-cost close range photogrammetry techniques for use in a variety of applications. The use of these techniques in medicine, forensic science, architecture, engineering, archaeology and anthropology to record, measure and monitor objects and sites has been growing in recent years. Close range photogrammetry has been particularly investigated and preferred for human body mapping due to being non-contact, non-invasive, accurate, and inexpensive and data is re-measurable.

Skulls have been traditionally measured using callipers and tape in anthropological study, which is subject to observer error. Close range photogrammetry can be used to perform more accurate measurements and retain a digital copy of the skull, which can be re-used for a number of purposes. Using low cost software (Photomodeler), and low cost cameras, the aim of this project is to detail the camera calibration techniques and image capture of a skull. The process for 3D modelling using close range photogrammetry includes camera calibration to determine the camera's internal parameters, photographing the object within a control target frame, and processing the data with photogrammetry software.

Achieving a high precision camera calibration and producing a high-accuracy 3D model were more difficult than anticipated. There are a number of factors which can result in a poor quality models. However, the results show that photogrammetry can be utilised in the capture of accurate 3D skull model using low-cost cameras efficiently. The research was successful, the project objectives were satisfied and the accuracy across the project was approximately 0.4mm.

Disclaimer

University of Southern Queensland
Faculty of Health, Engineering and Sciences
ENG4111/ENG4112 Research Project

Limitations of Use

The Council of the University of Southern Queensland, its Faculty of Health, Engineering & Sciences, and the staff of the University of Southern Queensland, do not accept any responsibility for the truth, accuracy or completeness of material contained within or associated with this dissertation.

Persons using all or any part of this material do so at their own risk, and not at the risk of the Council of the University of Southern Queensland, its Faculty of Health, Engineering & Sciences or the staff of the University of Southern Queensland.

This dissertation reports an educational exercise and has no purpose or validity beyond this exercise. The sole purpose of the course pair entitled “Research Project” is to contribute to the overall education within the student’s chosen degree program. This document, the associated hardware, software, drawings, and other material set out in the associated appendices should not be used for any other purpose: if they are so used, it is entirely at the risk of the user.

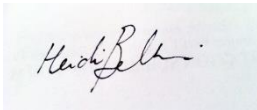
Candidates Certification

I certify that the ideas, designs and experimental work, results, analysis and conclusions set out in this dissertation are entirely my own efforts, except where otherwise indicated and acknowledged.

I further certify that the work is original and has not been previously submitted for assessment in any other course or institution, except where specifically stated.

Heidi Jane Belbin

Student Number: W0109098

A rectangular box containing a handwritten signature in black ink. The signature is cursive and appears to read 'Heidi Belbin'.

(Signature)

28/10/2015

(Date)

Acknowledgments

This project was carried out under the principal supervision of Dr. Albert Kon-Fook Chong, in which I express my sincere and greatest appreciation for his time and guidance in this project. I would also like to acknowledge Dr Glenn Campbell for his initial guidance in choosing a project.

I would like to express my appreciation to the Surveying and Spatial Sciences Institute (SSSI) for awarding me the Women in Spatial Scholarship 2015.

I am grateful to all who have helped and given me support during this project.

Table of Contents

Abstract	i
Disclaimer	ii
Candidates Certification.....	iii
Acknowledgments.....	iv
List of Figures	ix
List of Tables	x
List of Appendices	xi
Nomenclature and Acronyms	xii
1.0 Chapter One - Introduction	1
1.1 Outline of Study	1
1.2 Introduction	1
1.3 The Problem	2
1.4 Research Objectives	2
Objective 1: Camera Calibration	2
Objective 2: Image Acquisition.....	2
Objective 3: Data Processing and Creation of 3D Model	2
Objective 4: Accuracy of Results	2
1.5 Conclusion.....	2
2.0 Chapter Two - Literature Review	3
2.1 Introduction	3
2.1.1 Advantages of Close Range Photogrammetry for 3D Modelling.....	4
2.1.2 Potential Users of CRP for 3D Modelling.....	4
2.2 The Use of Close Range Photogrammetry for Human Body Mapping	6
2.2.1 Cranium	6
2.2.2 Teeth and Jaw	7
2.2.3 Foot.....	7

2.2.4 Hand.....	9
2.2.5 Spine	9
2.3 Complete Body Mapping	10
2.3.1 Forensic Applications	10
2.4 Movement Mapping	11
2.5 Camera Calibration	12
2.5.1 Camera Parameters	12
2.5.2 Calibration Methods	14
2.6 Photomodeler	15
2.6.1 Accuracy of Photomodeler	16
2.6.2 Applications for Photomodeler Software	17
2.6.3 Advantages and Disadvantages of Photomodeler	18
2.7 Summary	18
3.0 Chapter Three – Research Design and Methodology	20
3.1 Objectives.....	20
1. Camera Calibration.....	20
2. Image Acquisition.....	20
3. Data Processing and Creation of 3D Model	20
4. Accuracy.....	20
3.2 Implications of Research.....	20
3.3 Equipment	20
3.3.1 Cameras	20
3.3.2 Photogrammetry Software	20
3.3.3 Targets	21
3.3.4 Skull.....	21
3.3.5 Callipers and Tape	21
3.3.6 Miscellaneous	21

3.4 Camera Calibration	21
3.4.1 Target Type and Size	21
3.4.2 Calibration Method.....	22
3.4.3 Camera and Calibration Grid Position.....	22
3.5 Target Configuration	23
3.6 Image Acquisition	24
3.6.1 Texture of the Object.....	24
3.6.2 Lighting	25
3.6.3 Background.....	25
3.6.4 Camera Position and Angles.....	25
3.6.5 Camera Settings	26
3.7 Processing.....	26
3.7.1 Uploading Photos	26
3.7.2 Automatic Target Marking	26
3.7.3 Processing.....	27
3.7.4 DSM Trim.....	28
3.7.5 Create DSM	28
3.8 Creation of the 3D Model.....	29
3.9 Assessment of Accuracy	31
4.0 Chapter Four – Results and Discussion	33
4.1 Camera Calibration	33
4.1.1 Results of Calibration	34
4.1.2 Discussion of Calibration Results.....	35
4.2 Photograph Capture and Processing.....	36
4.2.1 Discussion of Model Results	37
4.3 Measurements and Accuracy	38
4.3.1 Skull Measurements	38

4.3.2 Check on Accuracy.....	39
4.3.3 Discussion of Results.....	39
4.3.4 Summary of Objectives Achieved.....	39
5.0 Chapter Five - Conclusions.....	41
5.1 Introduction.....	41
5.2 Conclusions.....	41
5.3 Further Research and Recommendations.....	42
References.....	43
Appendix A: Project Specification.....	47
Appendix B: Photodeler Referenced Material.....	48
Appendix C: Processing Report.....	49
Appendix D: Creating a 3D Dense Surface.....	53

List of Figures

	Page
Figure 2.1	The principle of photogrammetric measurement. 3
Figure 2.2	The effect of radial distortion on the lens. 13
Figure 2.3	Vertical misalignment of the camera lens. 13
Figure 2.4	Range of Photomodeler software. 16
Figure 3.1	Configuration of target camera positions and orientations. 22
Figure 3.2	Create Coded Targets window in Photomodeler. 24
Figure 3.3	Skull showing location of camera stations. 25
Figure 3.4	Automatic Target Marking options window in Photomodeler. 26
Figure 3.5	Processing options window in Photomodeler. 27
Figure 3.6	Photo configuration and Create Dense Surface options in Photomodeler. 29
Figure 3.7	Export options in Photomodeler and resulting DXF file in AutoCAD. 30
Figure 3.8	Screen shot of Photomodeler showing the Measurements pane. 31
Figure 3.9	Screen shot showing measurements between selected targets. 32
Figure 4.1	Overall RMS for all three sets. 33
Figure 4.2	Maximum residuals for all three sets. 33
Figure 4.3	DSM coloured with photo texture and single texture with points coloured with photo texture. 36
Figure 4.4	DSM with points coloured by depth, photo texture overlaid with point cloud, triangulated mesh and DSM showing close correlation with point cloud underneath. 36
Figure 4.5	DSM with comments. 37
Figure 4.6	Skull showing measurements mentioned in Tables 4.3 and 4.4 38

List of Tables

	Page
Table 2.1 A sample of papers which used PM in their research and stated the accuracy achieved.	17
Table 3.1 Indicators of quality in the processing report.	28
Table 4.1 Calibration sets completed and comments.	33
Table 4.2 Camera calibration results showing parameters, Root Mean Squared (RMS) and Maximum Residual	34
Table 4.3 Measurements taken on skull.	38
Table 4.4 Check measurements between targets.	39

List of Appendices

	Page
Appendix A Project Specification	47
Appendix B Photomodeler Referenced Material	48
Appendix C Processing Report (Raw File)	49
Appendix D Creating a 3D Dense Surface	53

Nomenclature and Acronyms

2D	Two Dimensional
3D	Three Dimensional
CBCT	Cone Beam Computed Tomography
CCD	Coupled Charged Diode
CMOS	Complementary Metal-Oxide Semiconductor
CT	Computed Tomography
CRP	Close Range Photogrammetry
MRI	Magnetic Resonance Imaging
PM	Photodeler
RMS	Root Mean Squared

1.0 Chapter One - Introduction

1.1 Outline of Study

This project involves testing the suitability and accuracy of low cost close range photogrammetry (CRP) for modelling a complex object, such as a human skull. Human skulls are important for the study of anthropology, archaeology, medicine, forensic identification to name a few applications. CRP is preferable to other methods of capturing data as it is low cost, accurate, non-invasive, non-contact, time efficient, photos and model are re-measurable, inaccessible spots can be photographed and able to be performed by professionals outside of the photogrammetry or spatial science field.

The project will assess the ease and simplicity of using Photomodeler to create a 3D model of a model human skull, as well as the accuracy attained. The Project Specification can be found in Appendix A.

1.2 Introduction

Low cost CRP is increasing in popularity as a method of capturing data to create accurate, true to scale 3D models of objects and scenes. There are a number of advantages of using CRP compared with other data capture methods, such as laser scanning. The advantages include:

- High accuracy
- Low cost
- Ease of use
- Portability
- Non-contact and non-invasive

The validity of the claims above as made by various research papers will be tested, by attempting to create a 3D model of a human skull using low cost CRP techniques, equipment and software, in which the following criteria will be assessed:

- Accuracy of camera calibration
- Quality of software processing (image to model quality)
- Ease of use
- Accuracy of the model
- Any problems or difficulties encountered

1.3 The Problem

Low cost CRP is becoming an increasingly widely used tool for capturing data for a range of applications. Photogrammetry software, such as Photomodeler, is marketed as being easy to use and can produce 3D models of high accuracy and quality. A complex object, such as a human skull, is an appropriate and real-world subject to test the ease at which a 3D model can be created using Photomodeler, as well as the accuracy which can be achieved by a non-professional (undergraduate student) using low cost equipment and basic photogrammetry techniques. There are difficulties in creating complex, 3D objects using CRP and methods for improving data capture are needed.

1.4 Research Objectives

Objective 1: Camera Calibration

Determine the most appropriate calibration for the task, including the coded target type, number of targets and discuss any differences between the two cameras.

Objective 2: Image Acquisition

Determine the optimal amount of targets to be used and configuration.

Objective 3: Data Processing and Creation of 3D Model

Analyse the level of difficulty and note any problems in the creation of the 3D model from the images.

Objective 4: Accuracy of Results

Assess the accuracy of the 3D model comparing measurements taken with callipers and tape.

1.5 Conclusion

This project aims to be a practical demonstration and a test of the accuracy that can be achieved using CRP techniques and a low cost, off the shelf camera in modelling a complex object, such as a human skull. During the case study, any difficulties during calibration, image acquisition and processing are to be noted and discussed. The literature review discusses advantages and problems researchers have experienced using low cost CRP and software for their particular applications. The case study in this project should help to uncover potential difficulties and good practice that may help to guide others in their use of low cost CRP.

2.0 Chapter Two - Literature Review

2.1 Introduction

The use of low cost CRP to create 3D models is a somewhat new tool, which has its roots in a longer history (Fryer, Mitchell & Chandler 2007, p. 1), that researchers in different professions are investigating the applications where CRP can be useful. CRP is becoming increasingly popular as a tool for data capture in fields outside of spatial science. For this reason it is important to investigate thoroughly how CRP has been used in a variety of applications and the appropriateness of the tool for the task. It is the role of spatial scientists to investigate technology and advise the professional community in the appropriate use and limitations of data.

The principles of photogrammetry involve the fundamental sciences of mathematics, physics, information sciences and biology. (Luhmann et al. 2006, p. 3) CRP has varied applications and a strong interdisciplinary character. (Luhmann et al. 2006, p. 3) A useful explanation of photogrammetry can be found in Luhmann et al. (2006, p. 2) and shown graphically in Figure 2.1 below:

“The primary purpose of a photogrammetric measurement is the three dimensional reconstruction of an object in digital form (coordinates and derived geometric elements) or graphical form (images, drawings, maps).”

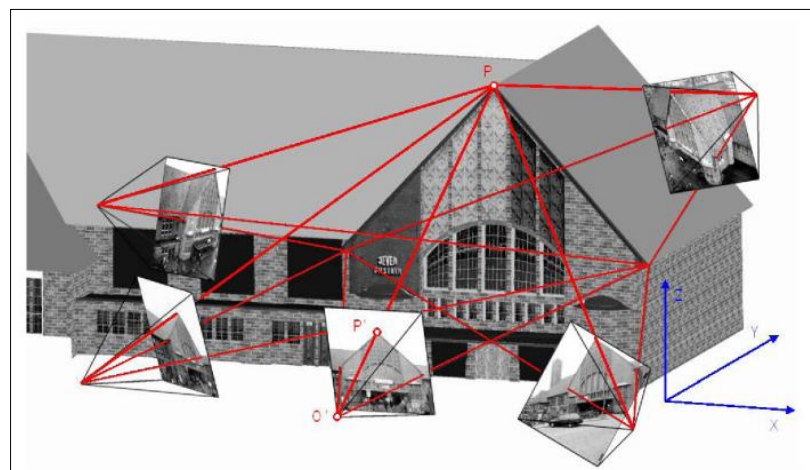


Figure 2.1 Taken from (Luhmann et al. 2006, p. 6) showing the principle of photogrammetric measurement.

There are many examples in the literature of the use of photogrammetry to record data, including examples of low cost CRP to record and map the human body. The literature review will highlight some uses focusing on CRP for human body mapping.

2.1.1 Advantages of Close Range Photogrammetry for 3D Modelling

The advantages of using photogrammetry to capture data includes (Majid et al. 2005, p. 55):

Non-invasive - Photogrammetry is able to be performed without making contact with the object to be modelled. Examples include capturing rock art and carvings which are inaccessible (on a high rock face) or fragile (Sanz et al. 2010); capturing data for a crime scene (Randles et al. 2010) or archaeological dig in which minimal contact with the site is preferred. (Sanz et al. 2010)

Instantaneous - Processing time can be minimal depending on the task and skill of the operator. (Majid et al. 2005, p. 55)

High accuracy - CRP has greater accuracy than using laser scanning. Laser scanning provides rapid 3D modelling, whereas photogrammetry provides precise measurement. (Galantucci, Percoco & Di Gioia 2010, p. 186)

Real world colour and texture - Photogrammetry software produces colour and texture from the photograph. (Majid et al. 2005, p. 55)

Permanent record - An accurate, scaled digital record of an object is important to preserve the characteristics of the object, which may be destroyed or fragile, for example a footprint. (Majid et al. 2005, p. 55)

Re-measurement possible if needed - It is possible to re-measure an object from photos and create models which can be re-measured as much as necessary by photogrammetry. (Randles et al. 2010, p. 8)

Cost effective – Low cost CRP is more cost effective than using other forms of survey equipment and can match or improve the quality of survey equipment. (Majid et al. 2005, p. 55)

2.1.2 Potential Users of CRP for 3D Modelling

There are a number of applications that can benefit from the use of CRP. Some examples include:

Anatomical Research

An example of use is the development of the Malaysian Craniofacial Database. Low cost but high accuracy facial and cranial models needed to be created particular to ethnic groups in Malaysia – Malay, Chinese and Indian – to determine normal variation in those populations for medical, forensic and anthropologic uses. (Majid et al. 2005, p. 49) Early homo crania can also be added to the data base for use in anthropology. (Chong et al. 2004, p. 17)

Surgery, Medicine and Dentistry

There is a wide variety of medical applications for CRP, including monitoring for disease, post and pre surgery assessment, and studies of motion. Photogrammetry has been used in dentistry to allow accurate models of teeth to be created to study bite contact in the jaw and teeth. (Shigeta et al. 2013) Detailed examples of the use of low cost CRP in the medical field are discussed later.

Forensic Science

Vehicle accident reconstruction is another application (Randles et al. 2010) and also crime scene investigation. (Chong et al. 2004, p.17) Photogrammetry allows a record of a crash or crime scene to be kept and re-examined at any time. (Randles et al. 2010, p. 8) Randles et al (2010, p.8) make the comment that photogrammetry has advantages over using a total station in that potential mistakes can be more easily seen and fixed; and that points can be missed when measuring using a total station, which are not noticed until the data is downloaded, making corrections difficult.

Archaeology and Heritage

CRP has gained popularity in archaeological research for applications such as recording, analysis, and creating accurate models of artefacts and rock faces (Sanz et al. 2010) and recording burial sites. (Dellepiane et al. 2013) ‘Analogue’ recording of artefacts is limited in the knowledge that can be displayed, including the ability to re-examine if the artefact should be destroyed or lost. (Krajňák, Pukanská & Bartoš 2011, p. 337)

It has also become a concern to give the general public access to archaeological and historical objects and sites in 3D, especially in this age of web technology and virtual reality. (Guarnieri, Pirotti & Vettore 2010) and (Krajňák, Pukanská & Bartoš 2011) Photogrammetry could help to provide data for those applications.

Architecture

CRP has become a tool for monitoring and recording heritage buildings and has applications within architecture as well. (De Reu et al. 2013) Hernán-Pérez et al. (2013) have examined the usage of a smart phone camera and CRP for architecture students to help learning within their field.

Engineering

Generally, the uses of CRP in engineering have involved the analysis of manufactured components, measurement of large structures and objects, to measure in difficult environments or perform on going measurements and testing of moving objects. (Fryer, Mitchell & Chandler 2007, p. 67)

2.2 The Use of Close Range Photogrammetry for Human Body Mapping

There are a variety of parts of the human body which have been mapped by CRP and a variety of uses for this data. The following are a selection of examples of mapping different parts of the human body.

2.2.1 Cranium

Three-dimensional modelling of the human skull has become an essential tool for those professions which study the human cranium. (Katz & Friess 2014, p. 152) Conventional techniques for measuring the skull and collecting data include the use of callipers, measuring tapes, compasses, protractors and angle finders. (Majid et al. 2005, p. 53)

Malaysian Craniofacial Database

An example of use is the development of the Malaysian craniofacial database. (Chong et al. 2004, p. 16) Low cost but high accuracy facial and cranial models needed to be created particular to ethnic groups in Malaysia – Malay, Chinese and Indian – to determine normal variation in those populations for medical, forensic, protective gear design and anthropologic uses. (Majid et al. 2005, p. 49) CRP was used to collect data, as well as other methods – laser scanning, cephalograms, dental casting and CT scans. (Chong et al. 2004, p. 17)

Skull Mapping

Katz and Friess (2014) studied the advantages of 3D modelling human skulls using photogrammetry and meshing the model with laser scanned data for anthropological purposes. CRP has the advantages of being low cost, portable, and quick and simple data collection possible but Katz and Friess (2014, p. 152) found that there were differences between the CRP and laser scanned models. It was also noted that finer details, such as teeth were problematic to model. (Katz & Friess 2014, p. 157)

Soft Tissue Facial Mapping

Ayoub et al. (2007) investigated the advantages in facial and cranial surgery of using a model of a patient's skull by CT scanning superimposed with a soft tissue facial model acquired by CRP. In previous years (in 2007), 2D images from photographs and radiographs were used to plan surgery and demonstrate changes in the face to patients pre surgery. (Ayoub et al. 2007, p. 242) Ayoub et al. (2007, p. 242) writes that it is challenging for the patient to visualise realistically changes in the frontal view of his/her face from 2D images of the lateral side of the face. CRP techniques are able to give the patient a realistic post-surgical view of the face with skin texture. (Ayoub et al. 2007, pp. 242-3)

Ayoub et al. (2007, p. 425) found that there were some errors associated with superimposing the facial model to the skull and mentions this was likely due to the effect of gravity on the cheeks, as the patients

were photographed in a supine position, and also the eyebrows and eyelids had errors which may be associated with facial expressions. Ayoub et al. (2007, p. 243) comments that CRP proved fast and of acceptable accuracy for their application.

Cevidane et al. (2010, p. S120) discusses the benefits of using cone beam CT to create 3D facial models to study soft tissue changes due to growth or treatment and they argue CRP and laser scanning are not suitable due to a lack of stable references for a changing face over time. Also, head position and facial expression cause difficulties, and light reflection from the eye lens interferes with the creation of the 3D model. (Cevidane et al. 2010, pp. S120-S1) Cevidane et al. (2010, p. S125) makes the comment that CT scans have a risk of exposure to radiation and risk of cancer, which CRP does not.

2.2.2 Teeth and Jaw

Photogrammetry has been used in dentistry to allow accurate models of teeth to be created to study bite contact in the jaw and teeth. (Shigeta et al. 2013) CRP has been demonstrated to be useful in monitoring normal and abnormal growth, malformations, surgical planning and evaluation of treatment in orthodontic surgery. (Galantucci, Percoco & Di Gioia 2010)

2.2.3 Foot

Modelling the foot can provide medical researchers and practitioners with valuable data for a variety of medical injuries and conditions. Al-Baghdadi et al (2011) examine the use of CRP to map the dorsal and plantar surfaces of the foot during weight bearing postures, which can be difficult to map. This information can be used in the design of foot wear and customised orthotics to suit the weight bearing dynamics of the foot, which shows more accurately the shape and pressure areas of a foot than models developed from an immobile, non-weight bearing foot. (Al-Baghdadi et al. 2011, pp. 295-6) Chong (2011) investigated the suitability of CRP for monitoring the hands and feet of CMT (Charcot-Marie-Tooth) disease patients for signs of muscle loss and reduced touch sensitivity.

Alshadli, Duaa et al. (2013) investigate CRP measurement of the foot to study links between foot posture in athletes and repetitive injury. Static and dynamic measurements were taken; static using a digital calliper and dynamic using CRP techniques. (Alshadli, Duaa et al. 2013, p. 2) It was found there were differences between the measurements of the static and dynamic postures of areas of the foot (arch), and comments made that it is important to consider changes in the foot during gait, not only the static measurements. (Alshadli, Duaa et al. 2013, p. 4)

Another issue in measuring a static foot using other techniques, such as radiographs, anthropomorphic measurements and foot print measurements, is determining the amount of weight bearing which causes changes in the morphology of the foot arch over the duration of the gait. (Alshadli, Duaa et al. 2013, p. 89) A “force plate” was set up, which works by matching a selected weight bearing amount (in percentage) to synchronise with a number of camcorders and then relates to a particular frame number, in which the foot morphology can be analysed. (Alshadli, Duaa et al. 2013, pp. 95-6)

Gait and Foot Movement Mapping

Al-Baghdadi et al (2011) constructed a glass top platform to capture the plantar and dorsal surfaces of the foot during movement using low cost video cameras. The materials used to construct a glass top platform are relatively cheap and maintenance is low and cost effective. (Al-Baghdadi et al. 2011, p. 301) CRP is advantageous compared to laser scanning to capture the data for the 3D model, as photogrammetry acquires the photographs instantaneously, whereas a scanner needs tenths of a second to capture points. (Al-Baghdadi et al. 2011, pp. 296, 301) There are also advantages over using a “flatbed scanner” to model the foot, as CRP can model the foot during gait with greater accuracy. (Al-Baghdadi et al. 2011, p. 296)

In their study, Al-Baghdadi et al (2011, p.301) encountered a number of difficulties using their CRP techniques to foot movement and gait. Mapping individual toes and edges of the foot was unsuccessful, due to holes appearing in the 3D surface. (Al-Baghdadi et al. 2011, p. 301) Different skin colour also affected the image capture, in which body paint was used to control the effects. (Al-Baghdadi et al. 2011, p. 301) Al-Baghdadi et al (2011, p.301) techniques are limited to walking as opposed to running or fast movements due to the frame rate of the video cameras.

When using a platform through which photographs are taken, a number of potential issues which may affect data quality need to be considered, and measures taken to minimise or eliminate these problems. It should be assessed whether there is any bending or flexing of the material when weight is placed on the surface. (Al-Baghdadi, Chong & Alshadli 2013, p. 262) Images can be affected by distortion from glass and plastic, and a further complication is that some materials have a uniform refractivity, whereas others exhibited non-uniformity. (Al-Baghdadi, Chong & Alshadli 2013, p. 262) This refraction causes outliers in the data of the foot being modelled. (Al-Baghdadi, Chong & Alshadli 2013, p. 262) Al-Baghdadi, Chong and Alshadli (2013, p. 274) studied the problem and found that the glass refraction values differed according to gait position and impurities in the glass.

2.2.4 Hand

Hoevenaren et al. (2015) investigate the suitability of CRP for producing 3D models of the hand, and focus their study of the repeatability of results from two observers selecting particular land marks on the hand for the model. The uses of CRP generated 3D models of the hand include planning surgery and a resource for teaching purposes. (Hoevenaren et al. 2015, p. 714) There is a gap in the literature for determining a complete list of soft tissue land marks on the hand, therefore, a list was compiled from different literary sources for use in their study. (Hoevenaren et al. 2015, p. 713) Hoevenaren et al. (2015, p. 714) comment that the fact that individual fingers can move independently of each other, may account for variances in land mark placement, whereas a face is limited in the amount different features can move.

Hoevenaren et al. (2015, p. 714), like Cevidanes et al. (2010, p. S125), mentions that CT scans and MRI expose patients to some radiation, which can be avoided using CRP and is more patient friendly due to being non-invasive. Results can be available in a shorter time frame than using CT and MRI and has lower associated costs. (Hoevenaren et al. 2015, p. 714) Hoevenaren et al. (2015, p. 714) mentions that a database of soft tissue hand data is needed for medical purposes, which could be combined with CT data for a 4D perspective on the hand for surgery and education.

2.2.5 Spine

Chong et al. (2009) examine the suitability for CRP to measure changes in the spine's contours by conducting a study to test the expected diurnal variation of the spine in a sample of 30 males using CRP. The results were then compared to data collected using a stadiometer presented in other studies. (Chong et al. 2009, p. 270)

Traditionally, spinal measurements are taken with the use of a stadiometer, which has some disadvantages, including the sheer size of the instrument. (Chong et al. 2009, pp. 265-6) These disadvantages can be overcome by the use of CRP, namely, unlike a stadiometer, it is non-invasive, acquires all measurements instantaneously, able to measure landmarks of the spine with high accuracy and create a digital record of the measurements. (Chong et al. 2009, p. 266)

2.3 Complete Body Mapping

2.3.1 Forensic Applications

Autopsy Records

Urbanová, Hejna and Jurda (2015) investigate the benefits of both CRP and laser scanning to document autopsies. Three dimensional modelling is useful for the documentation process as re-measurement and analysis can be made in the future. (Urbanová, Hejna & Jurda 2015, pp. 77-8) This is particularly relevant to being able to reassess body measurements, wounds, angles of penetration of weapons and so on. (Urbanová, Hejna & Jurda 2015, p. 78)

In their paper, Urbanová, Hejna and Jurda (2015, pp. 78, 83) commented that CRP in particular was appealing as it is simple, inexpensive with relatively trivial equipment needs and can be performed without “special training” or “prior experience.” However, when discussing the results of their case study, scanning and using CRP to create 3D models of two deceased individuals and one living person, a number of difficulties were encountered with both techniques. (Urbanová, Hejna & Jurda 2015, p. 84)

In regards to CRP, the model had “scrappy edges” where the bodies touched the autopsy table and in the living person’s model, there were differences due to body movement, such as breathing. (Urbanová, Hejna & Jurda 2015, p. 84) There were also some holes in the model due to body hair, depressions and body fluids, in regards to the images taken when the deceased bodies were opened for examination. (Urbanová, Hejna & Jurda 2015, p. 85)

Despite these challenges, the CRP derived models showed the entire surface of the body including areas of greater error, whereas the scanner algorithm will not generate those areas of high error. (Urbanová, Hejna & Jurda 2015, p. 85) CRP was also able to document in photo-realistic texture the skin, any blemishes, scars, injuries and tattoos, better than the scanner. (Urbanová, Hejna & Jurda 2015, p. 84) Urbanová, Hejna and Jurda (2015, p. 86) comment that CRP is a useful tool to document post mortems, but the amount of time needed to process a full body may not be desirable, and that CRP is better for documenting areas of interest on the body.

Slot, Larsen and Lynnerup (2014) also investigated the benefits of CRP in autopsies, focusing only on physical measurements of the body, such as measuring the location of wounds. Usually when performing an autopsy, “areas of interest” on a body, such as wounds, are described in text and photographed, with measurements of size recorded and location described in relation to a particular anatomical point. (Slot, Larsen & Lynnerup 2014, p. 226)

Further information can sometimes be required after the autopsy, which then is impossible to collect or re-measure, which is the reason CRP is beneficial to forensic applications, as a 3D model can be repeatedly re-measured and studied. (Slot, Larsen & Lynnerup 2014, p. 226) Slot, Larsen and Lynnerup (2014, p. 228) found that the differences between body measurements using a ruler and using photogrammetry were less than 1cm, which is in an acceptable range for body measurement purposes.

2.3.2 Height Estimation

A person's height can be estimated using images and photogrammetry techniques and this is particularly useful in criminal investigations. Chong (2002) discusses a technique of calibrating surveillance cameras in situ using a portable target control frame to be able to extract measurements of suspect's height, which can be used to identify a person. This technique is not limited to a person height; it can be used to measure other parts of a body, such as an arm or even a shoe to estimate shoe size. (Chong 2002, p. 758) Chong (2002, p. 758) writes that the average accuracy of using this technique was 23mm +/- 7mm.

Hoozeboom, Alberink and Goos (2009, p. 1365) examine the issue of differences between the real height of a person and the height derived from the images to examine what is the cause of these differences. In their paper they write that there is a correlation between the camera view side used to estimate height, the type of camera and the height calculated. (Hoozeboom, Alberink & Goos 2009, p. 1373) Hoozeboom, Alberink and Goos (2009, p. 1375) also comment that the stance of the person when the height measurements are calculated has an effect on the accuracy of the value.

2.4 Movement Mapping

Low cost video cameras are able to be used to capture human movement using photogrammetric techniques and software. (Chong 2006, p. 227) There are a wide variety of uses for this kind of data, including medical applications, such as the foot and gait during walk, discussed previously.

Chong (2006) conducted a study to examine the propulsion of the hand for application in swimming. CRP was deemed to be useful to this study as photos of the hand during motion can be captured instantly of both sides of the hand in a multi camera set up, and can be operated underwater. (Chong 2006, p. 74)

2.5 Camera Calibration

Calibration is one of the most debated problems in photogrammetry. (Galantucci et al. 2014, p. 279) Low cost, consumer grade, non-metric cameras are designed for the purpose of photography and need to be calibrated for photogrammetry usage. (Hassan, Ma'Arof & Samad 2014, p. 123) Calibration calculates parameters related to the position and rotation of each camera in the 3D space (external parameters), the focal length and position of the principal point on the sensor (internal parameters), lens distortion and non-symmetrical components. (Galantucci et al. 2014, p. 280) Another way of explaining basically what camera calibration aims to achieve, is to quote Hassan, Ma'Arof and Samad (2014, p. 124), “The purpose of camera calibration is to distinguish wholly the light rays when it was exposed when entering the camera.”

2.5.1 Camera Parameters

The geometric configuration inside a camera and its lens system is referred to as the *interior orientation* of the camera. (Fryer 2001, p. 156) As a lens is never perfect, these imperfections result in a reduction of image quality and error in the location of the image. (Fryer 2001, p. 157) Radial and decentring distortion relate to the lens of the camera and affect the location of the image. (Fryer 2001, p. 157)

Format Size

A format size refers to the size (area) of a camera's imaging chip (CCD or CMOS) which affects the imaging area of the camera. (EoS Systems Inc. 2015)

Focal Length

Photomodeler provides a simple and useful explanation of focal length, “...the distance between the imaging plane (e.g. the image chip in a digital camera) and a point where all light rays intersect inside the lens (the ‘optical centre’).” The principal distance relates to the focal length in that the focal length is the principal distance when the lens is focus is to infinity. (EoS Systems Inc. 2015)

Principal Distance

The principal point is the distance between the centre of the camera lens and image plane. (Fryer 2001, p. 158) According to Fryer (2001, p. 158), an approximation of the principal distance and a calculated value for the coordinates of the image and real world object are satisfactory to obtain the principal distance for the camera.

Principal Point

The principal point, or the full term, the principal point of autocollimation, refers to the point at which the true centre of the lens would project in a straight line to the image plane. (Fryer 2001, p. 158) The

lens centre is often located imperfectly, thus the focal plane not truly perpendicular to the optical axis, in which the calibration process will determine the misalignment error and position of the principal point. (Fryer 2001, p. 158)

Radial Distortion

Radial distortion can be described as *barrel* or *pin cushion* in nature, and can be best demonstrated by the shape of a rectangle which will appear distorted depending on whether it is located closer or further from the principal point. (Fryer 2001, p. 159) Figure 2.2 (below) shows the effect radial distortion has to the lens of the camera.

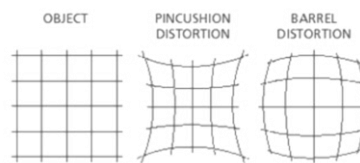


Figure 2.2 The effect of radial distortion on the lens (Yusoff et al. 2014, p.2)

Radial distortion can be calculated by the formula:

$$\delta_r = K_1 r^3 + K_2 r^5 + K_3 r^7 + \dots$$

where K_1 , K_2 , K_3 are coefficients and δ_r (radial distortion) is in micrometres (μm). (Fryer 2001, pp. 160-1)

Decentring Distortion

Decentring distortion refers to the vertical or rotational displacement of images caused by misalignment in the lens of the camera. (Fryer 2001, pp. 162-3) Figure 2.3 (below) shows what is meant by vertical misalignment of a camera lens. Decentring distortion is also affected by changes in pressure, vibrations or shock. (Fryer 2001, p. 164)

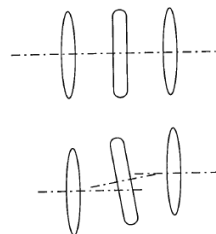


Figure 2.3 Vertical misalignment of the camera lens. (Fryer 2001, p. 163)

2.5.2 Calibration Methods

There are a few methods of camera calibration, which include analytical plumb line, field calibration, system calibration and self-calibration. Traditionally, calibration was achieved by the use of coordinated targets measured and calculated using theodolites or images acquired from metric cameras, in a laboratory setting. (Fryer 2001, p. 165) As CRP has progressed, there is a need for practical, inexpensive and time efficient calibration methods. (Fryer 2001, p. 165)

Analytical Plumb Line

Analytical plumb line calibration can determine radial and decentring distortion but cannot determine the principal point or principal distance. (Fryer 2001, p. 168) Its usefulness is often seen as an independent check for other calibration methods or to ascertain lens distortion trial values for a bundle adjustment. (Fryer 2001, p. 168) Analytical plumb line calibration involves photographing straight lines, which may be constructed from fishing line for example, and examining the departure from this straight line in the image. (Fryer 2001, p. 168) This departure from object to image represents lens distortion. (Fryer 2001, p. 168) A number of points are observed and mathematical formulae are used to derive values for the parameters x_p , y_p , K_1 , K_2 , K_3 and P_1 , P_2 . (Fryer 2001, p. 168) The obvious disadvantage of using analytical plumb line calibration is that it is incomplete on its own; it cannot solve for principal distance and the principal point.

Field Calibration

Field calibration (or sometimes referred to as 'on-the-job calibration) involves placing targets which can be used for calibration around the object to be measured or modelled at the time of photo acquisition. (Fryer 2001, p. 166) Survey equipment is often utilised to ensure control targets are placed accurately. (Fryer 2001, p. 166) Field calibration can be advantageous to other calibration methods where the focus of the lens needs to be changed during the photo set. (Fryer 2001, p. 166)

System Calibration

The term system calibration refers to calculating all parameters, both internal and external of a complete measurement system. (Luhmann et al. 2006, p. 453) System calibration is usually used for the calibration of multi camera systems, either fixed in position or movable. (Luhmann et al. 2006, p. 453) The exterior parameters can be determined by the use of reference points, and checked by a bundle adjustment or spatial resection. (Luhmann et al. 2006, p. 453) The interior parameters can be determined by object fields and object points with appropriate geometry. (Luhmann et al. 2006, p. 453)

Self-Calibration

Self-calibration is the most commonly used method of calibrating low cost, off the shelf, digital cameras for photogrammetry applications. (Udin & Ahmad 2011, p. 138) Alshadli, Duaa et al. (2013, p. 91) comment that self-calibration is the most effective technique, as coordinates of high accuracy are not necessary and, additionally, the bundle adjustment solves both the interior orientation parameters of the camera and the exterior position of each camera.

Calibration methods using 3D calibration objects produce more accurate results provided that the calibration object has targets placed in an optimal configuration. (Samper et al. 2013, p. 118) However, 2D calibration grids are easier to use and low cost compared to purchasing 3D complex objects, and, importantly, for many projects the accuracy that can be obtained by 2D grids is more than satisfactory for the application. (Samper et al. 2013, p. 118)

Self-Calibration Methodology

Udin and Ahmad (2011) examine the suitability of three different types of cameras for CRP applications by testing the accuracy and precision of each using the self-calibration bundle adjustment method. In their study, Udin and Ahmad (2011, p. 140) list a number of factors which can influence the results of a calibration: lighting, distance between the camera and calibration grid, position of the camera, camera resolution and pixel size. The camera should be rotated 90° to measure the principal point. (Udin & Ahmad 2011, p. 138)

Bundle Adjustment

A bundle adjustment is used to mathematically solve the calibration parameters. Alshadli, Duaa et al. (2013, p. 91) use simple terms to explain what a bundle adjustment does, “The bundle adjustment process involves taking multiple convergent images of a pre-calibrated targeted grid from different angles and views and the imaged targets are used to create a resection-intersection of the bundle of rays based on the co-linearity condition...” This process is performed during the processing of a calibration, such as using software such as Photomodeler or Australis for example.

2.6 Photomodeler

Photomodeler by EoS Systems Inc. is one of the cheaper photogrammetry software packages on the market, which describes itself as being able to achieve high accuracy for a range of applications. There are three kinds of Photomodeler software: Photomodeler, Photomodeler Scanner and Photomodeler Motion. (See Figure 2.4) The website (EoS Systems Inc. 2015) also contains a substantial amount of

information including the basics of how photogrammetry works, a ‘knowledge base’ of technical support and examples of how PM can be used for various applications. This information is all freely available online. A list of useful articles can be found in Appendix B. The software package also contains tutorials with videos which are simple and help to perform a calibration and create a Dense Surface Mesh (DSM) of an object or scene. Targets and calibration sheets can be printed using the program.

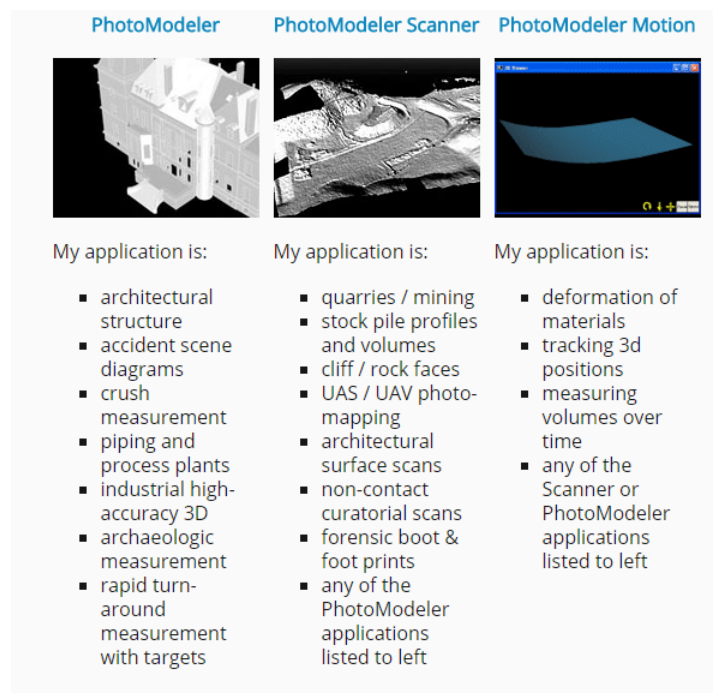


Figure 2.4 Range of Photomodeler software (EoS Systems Inc. 2015)

2.6.1 Accuracy of Photomodeler

Photomodeler states that the accuracy which can be achieved by PM is dependent of a number of factors, including (EoS Systems Inc. 2015):

- Resolution of photos
- Number of photos used for a model
- Angles between photos
- Number of referenced points
- Quality of the camera

PM quotes low resolution accuracy to be 1:200 to high resolution accuracy 1:8000. (EoS Systems Inc. 2015)

The accuracy obtained by the selected papers in the literature using PM can be seen in Table 2.1 (Below). Differences between the accuracy results varies, however, it is important to acknowledge differences are dependent on the objects modelled, distances of the object to camera, the cameras used for each project and the skill and experience of the operators. Table 2.1 provides an overview of the range of accuracy which others have achieved using PM. As seen below, it is possible to achieve sub-millimetre accuracy using PM.

Author of Paper	PM Product	Application	Accuracy
(Al-Baghdadi et al. 2012)	PM Scanner	3D modelling of a human foot	0.250mm – model surface 0.015mm between targets
(Galantucci et al. 2014)	PM Scanner 6.0	Mannequin faces	0.126mm
(Green, Matthews & Turanli 2002)	PM Pro	Underwater site mapping	2.3mm – 2.9mm
(Hernán-Pérez et al. 2013)	PM	Sculpture	10mm
(Oniga & Chirilă 2013)	PM Scanner	Sphere	0.007mm – 0.38mm
(Percoco, Galantucci & Lavecchia 2011)	PM	Mannequin torso	1.5mm – 4.5mm
(Rahman & Alam 2013)	PM Pro 4.0	Human faces	1mm
(Randles et al. 2010)	PM	Damaged cars (accidents)	2mm ±1.4%
(Lynnerup, Andersen & Lauritsen 2003)	PM	Mannequin	<10mm

Table 2.1 A sample of papers which used PM in their research and stated the accuracy achieved.

There are also many papers in the literature which do not state the accuracy achieved through their research, and this is more common of researchers investigating the use of CRP for their particular applications who are new to the technology. This perhaps indicates that spatial professionals should be more involved in projects to advise non-spatial researchers how to use the technology appropriately and be able to assess the accuracy of their data.

2.6.2 Applications for Photomodeler Software

The applications for PM are widely varied and include (EoS Systems Inc. 2015):

- Accident Reconstruction & Forensics
- Archaeology
- Architecture & Preservation
- Biology
- Engineering
- Film, Gaming and Animation
- Geology

- Surveying
- UAS / Drones

2.6.3 Advantages and Disadvantages of Photomodeler

Al-Baghdadi et al. (2011, p. 297) in their study of mapping the human foot chose to use PM Scanner to create 3D surface models of the foot because of PM's capability for DSMs and the ability to export point clouds and triangulated meshes in a variety of formats for further analysis and manipulation. Al-Baghdadi et al. (2011, pp. 298-9, 302) made a number of observations about how PM performed for their study:

- Black and white circular targets were captured by PM with greater accuracy than other colour combinations.
- A depth range was assigned to allow quicker processing and matching of the images to create the DSM.
- The foot needed to be painted with a matte red body paint to ensure uniform accuracy across the DSM.
- Individual toes were difficult to map due to being close together.

Galantucci et al. (2014, p. 288) remarks that the algorithm used for sub-pixel marking (recognising points) in PM Scanner recognises these points by contrast. Points located laterally on a surface are marked with an ellipse which results in a loss of precision. (Galantucci et al. 2014, p. 289) However, for the application of clinical studies of body surfaces, PM provides a sufficient level of accuracy and reliability. (Galantucci et al. 2014, p. 290)

Some of the points mentioned above are common remarks throughout the literature about CRP in general and are not necessarily particular to PM software itself.

2.7 Summary

The literature review reveals that CRP has many advantages over other technologies in 3D mapping, especially mapping the human body, fragile or inaccessible objects. The advantages include being non-invasive, instantaneous, highly accurate, real world colour and texture, creation of a permanent record, re-measurable and cost effective. Many of these characteristics are particularly useful for human body mapping.

While there are many advantages to using CRP for human body mapping, there are some common problems in the literature, such as difficulty in modelling fine details, such as teeth and toes. Also, where an object or body area touches a surface, like a table, holes can form in the 3D model. Modelling hands or faces can produce inaccuracies due to movement of individual fingers or facial expressions. Some researchers had difficulty combining data from CRP with other data capture techniques, such as CT scans.

The calibration process is necessary for non-metric cameras designed for photography rather than photogrammetry. The parameters which need to be determined by calibration include format size, focal length, principal distance, principal point, radial distortion and decentring distortion. There are a few different calibration techniques which can be used. The most appropriate for a low cost, off the shelf digital cameras is self-calibration using a bundle adjustment to determine the parameters.

Researchers have produced accurate results using CRP and Photomodeler, including human body mapping. In a sample of papers which used Photomodeler, accuracies varied between 0.007mm to 10mm across a wide variety of applications.

3.0 Chapter Three – Research Design and Methodology

3.1 Objectives

1. Camera Calibration

Determine the most appropriate calibration for the task, including the coded target type, number of targets and discuss any differences between the two cameras.

2. Image Acquisition

Determine the optimal amount of targets to be used and configuration.

3. Data Processing and Creation of 3D Model

Analyse the level of difficulty and note any problems in the creation of the 3D model from the images.

4. Accuracy

Assess the accuracy of the 3D model using measurements taken by callipers and tape.

3.2 Implications of Research

It is intended that the outcome of this project will add to the knowledge base of the uses and effectiveness of low cost CRP to model complex objects. Also, analysis and discussion of any difficulties will be useful to determine how easy it is to create an accurate model. It may help students and researchers in the future to determine if low cost CRP is suitable to apply to their particular task.

The impacts of this project are negligible, especially since the decision was made to use a model human skull instead of a real one. If a real human skull was to be used, ethics would have needed to be considered.

3.3 Equipment

3.3.1 Cameras

The cameras selected for the task are both Nikon S3700 (20.1 Megapixels), which are commonly available and priced at \$135.00 each at the time of purchase (May 2015).

3.3.2 Photogrammetry Software

The photogrammetry software selected is Photomodeler, priced at approximately \$5000 (Al-Baghdadi et al. 2011, p. 301) Photomodeler was selected as it is one of the cheaper, user friendly software packages on the market and USQ was able to lend a licence for the duration of the project at no cost.

3.3.3 Targets

Targets are available as part of the Photomodeler Scanner software package to be printed and used.

3.3.4 Skull

It was originally proposed to use a real human skull for the project, but it was not possible to arrange access. Alternatively, a high quality, cast model was used.

3.3.5 Callipers and Tape

A good quality Sidchrome digital calliper was purchased, 0-200mm, graduation: 0.01mm, model: SCMT26116. A good quality 3m Stanley tape was also purchased.

3.3.6 Miscellaneous

A number of materials are available for use in the lab to create an appropriate background for the photograph acquisition, such as black cardboard, frame, sticky tape etc. Also, other resources are available, such as measuring tapes, scale and tripod. A painted photo frame was used for a control target frame off campus.

3.4 Camera Calibration

A number of steps are required in the calibration process:

1. Select target type and size.
2. Choose method, single sheet or multi sheet calibration.
3. Decide position of camera and target sheet.
4. Capture a set of images.
5. Process the calibration using Photomodeler software.
6. Analyse the results.

3.4.1 Target Type and Size

The targets selected for the calibration are available to print in the Photomodeler software. To print calibration sheet, go to *File – Print Calibration Sheet(s)...* This type of target is recommended for small-scale projects, such as a car or foot print. (EoS Systems Inc. 2013, Ch.3) The target grid sheet, known as a “Calibration Sheet” in the Photomodeler Tutorials, was printed to A3 size; a size which covers the size of the skull. (See Image 3.1 below)

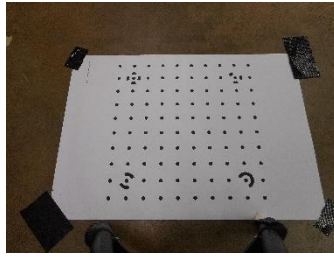


Image 3.1 Calibration grid from Photomodeler

3.4.2 Calibration Method

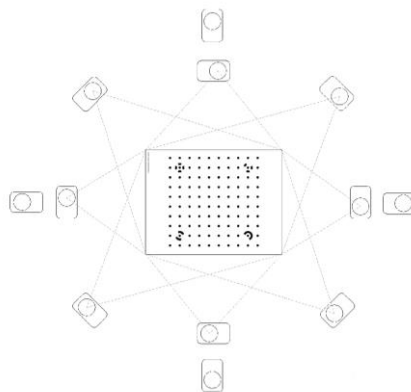
A single sheet calibration method was used, which is recommended for small scale projects. (EoS Systems Inc. 2013, Ch.3) This involves photographing a single sheet (as pictured in Image 3.1) from different angles and camera orientations, as recommended by Photomodeler. (EoS Systems Inc. 2013, Ch.3) The Calibration Sheet was placed on the floor and fastened with sticky tape to remain flat and prevent movement.

3.4.3 Camera and Calibration Grid Position

A total of twelve photographs were taken of the Calibration Sheet, see Figure 3.1 below. As seen from Figure 3.1, eight photographs were taken from each side of the sheet, four in portrait orientation and four in landscape orientation of the camera. An additional four were photographed from the corners, in either portrait or landscape orientation. This procedure is recommended by Photomodeler. (EoS Systems Inc. 2013, Ch.3)

There was a problem in the initial attempts of processing the calibration in PM at the USQ Laboratory, due to the organisation of the calibration photos. If the photos for each calibration set are not saved in separate folders, the calibration will experience problems which will only become evident when attempting to process photos for the model in PM. It is important that directories for calibration sets are kept separate and organised.

Figure 3.1 Configuration of target camera positions and orientations.



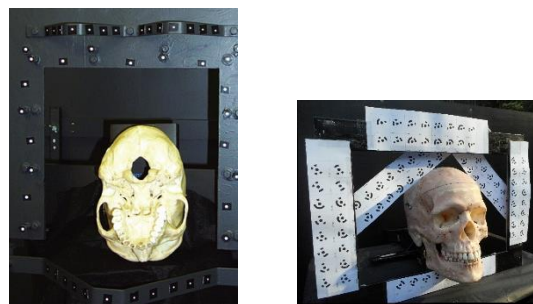
3.5 Target Configuration

The placement of targets either around the object, on the object or both are an important consideration, as it does affect the outcome of the photograph processing. In the Photomodeler tutorials (EoS Systems Inc. 2013), there are examples of different objects being photographed. Some use only targets surrounding the object, while others place targets on the object.

Numerous configurations were trialled, both with targets surrounding the skull and targets stuck onto the skull. The success of the photo acquisition and DSM creation appears to be somewhat correlated with the number of targets used, among other factors (discussed later). The target configuration aims to orientate the image and provide a fixed point for the modelling.

A target frame was constructed using a photograph frame painted black and the targets were fixed onto the frame by sticky tape, as glue tended to make the target paper strips bubble. Even sticky tape caused the paper target strips to lose tension in time, which is an important consideration if a target frame is intended to be used over an extended period of time. The inspiration was taken from Majid et al (2005, p.57) and the result, shown in Image 3.2 below.

Image 3.2 (Left) Majid et al (2005, p.57) and (Right) Frame constructed for project.



Target Type

The targets used were 12 bit coded targets, available for printing from the Photomodeler software. To create Coded Targets using PM, go to ***File – Create Coded Targets...*** (See Figure 3.2 below) These targets were selected due to the number of unique targets in the set (96), which were an appropriate number to be sufficient for the task. The colours selected were a white background with a black target, as this is easy to print and assumed easier for Photomodeler to recognise during the Automatic Target Marking function, as mentioned by Al-Baghdadi et al. (2011, p. 298).

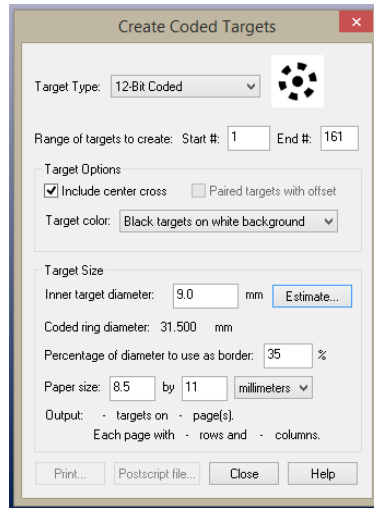


Figure 3.2 Create Coded Targets window.

3.6 Image Acquisition

The success of the image acquisition is not known until the images are processed in Photomodeler. The specifics of the processing will be discussed later but this section will discuss various factors needed for consideration when photographing the object.

3.6.1 Texture of the Object

The texture of objects affects the success of the photo acquisition. The Photomodeler website contains an article which writes that smooth and matte textures, such as plasterboard, do not work well, whereas textures such as soil and rock, with random patterns and colours work the best. (EoS Systems Inc. 2015) The skull's original texture was smooth and this is believed to have caused some difficulty. A successful DSM was created of the original texture but targets needed to be stuck onto the skull itself. To test whether texture was causing DSM creation problems, the skull was lightly tinted with a water-based acrylic paint (a red-brown colour). The DSM colour represents the painted colour more accurately than the unpainted skull. See Image 3.3 below.



Image 3.3 Original skull (left) and after paint applied (right)

Other methods of introducing texture to the skull were also tried, such as dusting with talcum powder, dirt and foundation powder make-up, but these were unsuccessful in creating a DSM. Powder and paint are recommended by Photomodeler (EoS Systems Inc. 2015) and Al-Baghdadi et al. (2011) also used paint for better results of creating DSMs of feet. Real bone textures, especially weathered or old specimens, would perhaps perform better due to having a more random surface texture.

3.6.2 Lighting

The lighting was considered as a possible cause of difficulties, as Alshadli, Duaa et al. (2013) had problems with glass and Cevidanes et al. (2010) with the iris of the eye. PM also recommends consistent lighting across photos to improve textures. (EoS Systems Inc. 2013, Ch.2-3) The aim of lighting is to decrease shadow and contrast between the image and the background to ultimately improve DSM results. The problem with photographing indoors is that the lighting is likely to be dull. Using lights often adds shadow to the photos and it proved difficult to press the button on the camera to take the photo without making shadows on the skull. Photographing in natural light appears to produce better quality, evenly coloured and realistic textured photographs without shadow.

3.6.3 Background

The background of the object is also important. When a background is not used, there are many unwanted points and noise captured in the photo. When the skull was photographed without a background, the Automatic Target Marking function in PM would mistakenly identify texture in the background as a target, especially if the image capture was outside (with trees and randomly textured earth in the background). A black background was used so that light would not be reflected and would not appear shiny, the skull would contrast with the background and the targets would be distinctive. A black background was used in CRP image capture of the skulls for the Malaysian Craniofacial Database. (Majid 2005).

3.6.4 Camera Position and Angles

If the camera is placed at an acute angle, the targets will not be recognised by the Automatic Target Marking process, which occurred in some of the unsuccessful attempts. Keeping the photos at a moderate angle yields better results. Also, positioning the camera so that the control frame and skull are contained in a large portion of the photo improves the result. Figure 3.3 below shows the different camera positions (represented by blue squares) to capture the images of the skull.

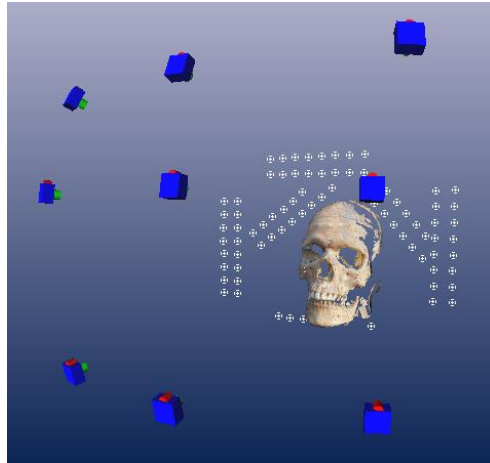


Figure 3.3 Skull showing location of camera stations

3.6.5 Camera Settings

Another issue to consider is a particular camera's default settings, which may come into effect each time the camera is switched on or off. For this project, each time the camera was used the flash was switched off and the zoom checked to ensure it was fully zoomed out, as the flash in particular automatically is enabled each time the camera is powered on and off.

3.7 Processing

Appendix D outlines the steps taken to create the DSM model. This section will detail specific selected settings used for discussion.

3.7.1 Uploading Photos

Photos can be uploaded to Photomodeler and automatically oriented using the step by step process. It is important not to orientate, crop, or modify the photos in any way otherwise the project will not process. (EoS Systems Inc. 2013, Ch.5) For reasons unknown at this stage, the Red camera used to capture the photos for the model sometimes orientated landscape photos 90° and when modified to the correct orientation before uploading to PM, the processing was unsuccessful.

3.7.2 Automatic Target Marking

The Automatic Target Marking function in PM recognises targets automatically in each photo. This process is able to be performed manually (EoS Systems Inc. 2013, Ch.5), however, the automatic function saves a significant amount of time, especially if there are many targets. Figure 3.4 below shows the various settings and options which can be selected for the operation.

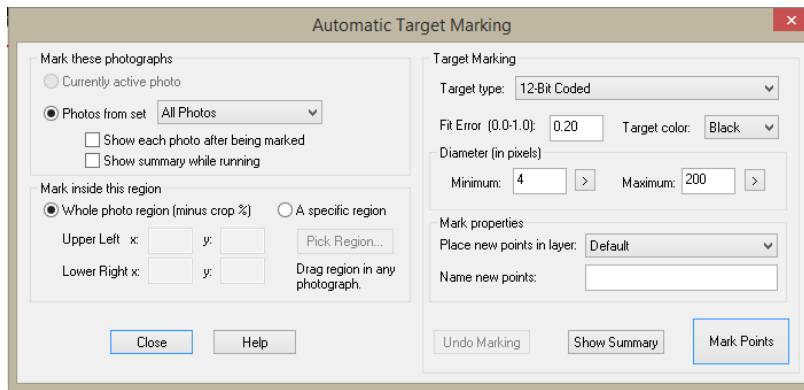


Figure 3.4 Automatic Target Marking options.

Two issues occurred with this operation. Firstly, when targets are printed for use, they are unique and numbered accordingly, for example, in 12-bit there are 96 targets. If a few sets of targets are printed, it is important not to use two identical targets in the photo, as the photos will not be oriented and automatic targeting will not work. Secondly, targets may not be identified if there is too much shadow in the photo or if there are objects in the photo which may be confused with a target.

3.7.3 Processing

Default options were accepted and the project was processed. See Figure 3.5 below.

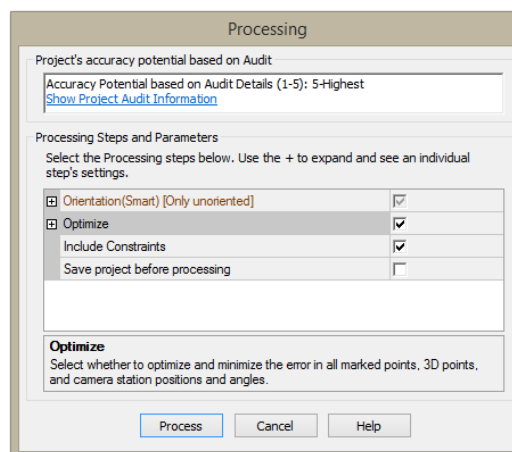


Figure 3.5 Processing options.

A report can be saved as a text file which contains useful data which indicates the quality of the processing outcome. Some useful indicators of quality contained in this report are listed in Table 3.1. (See Appendix C for full report) Tables can also be generated through the *View* menu, which can list a more comprehensive list of parameters and results.

Quality Indicator	Result	Comment
Number of photos oriented	9	Good result, all photos have been oriented
Bad Photos	0	
Weak Photos	0	
OK Photos	9	Good results, all photos are acceptable
Average Photo Point Coverage	50%	80% + is best
Point Marking Residuals		
Overall RMS	0.819 pixels	Satisfactory result, RMS <1.0
Maximum RMS	1.667 pixels	
Minimum RMS	0.324 pixels	

Table 3.1 Indicators of quality in the processing report.

3.7.4 DSM Trim

A DSM Trim is performed so that the process will be more streamlined, only creating DSM for the area in the selection; it is similar to cropping a photo. For this project, it was sufficient to trim reasonably close to the skull to create the DSM, similar to the steps outlined in Tutorial 2 of the footprint. (EoS Systems Inc. 2013, Ch.5) Some examples highlighted on the PM website trim as close to the object as possible. (See Appendix B, Animal Skull Scan)



Image 3.4 DSM Trim of the skull. (Lines surrounding skull)

3.7.5 Create DSM

Creating a successful DSM was initially problematic. Two possible sources of difficulties which could be manipulated through changing defaults were examined in order to improve the DSM. Firstly, instead of using the option *All Photos (MVS)*, the option of *Paired photos* was used. (See Figure 3.6 (right) below) This allows specific pairs of images to be selected and used to create the DSM. For

example, Figure 3.6 (left) below shows the sequence in which the photos were taken. In this case, paired photos 1-2, 1-4, 2-3, 2-5, 3-6, 4-5, 4-7, 5-6, 5-8, 6-9, 7-8, and 8-9 would be selected for use.

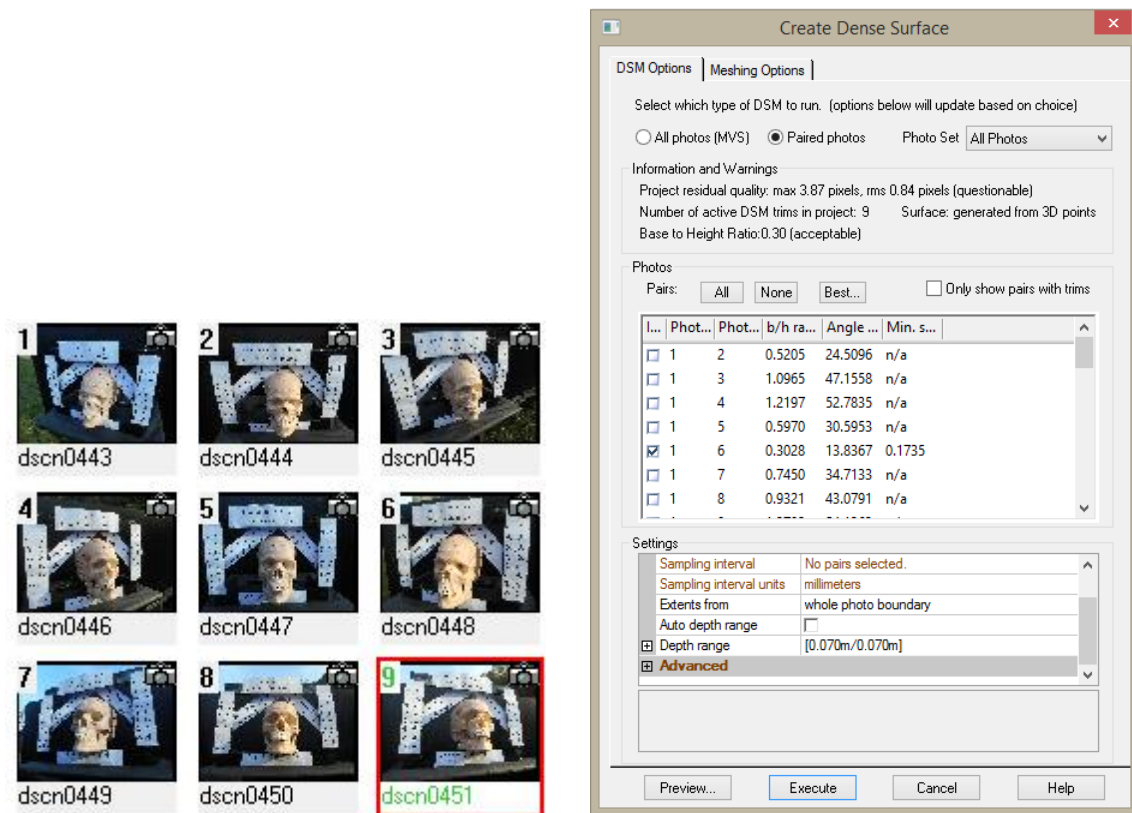


Figure 3.6 Photo configuration (left) and Create Dense Surface options (right).

Secondly, *Auto depth range* was de-selected, which allows a value to be entered which limits the depth used to create the DSM. A value of 700mm was entered, which was more than enough depth to contain the all parts of the skull. When *Auto depth range* was selected in the first attempts of DSM creation in the USQ laboratory, the auto depth calculated was too large and the background objects were causing difficulty to the DSM and also creating noise (unwanted points) in the model.

In all other options, default settings were accepted. As discussed earlier, the target configuration and image acquisition play a significant part in the success of the DSM. Mainly through trial and error and also consulting the literature, the problems could be solved.

3.8 Creation of the 3D Model

The original plan for creating a DSM of the skull for this project was to create a complete 360° model through combining the DSM faces of the skull. However, due to the amount of difficulties experienced

during the project, which impacted on time, a single frontal face DSM was created. The single face is still able to be used for taking measurements and the accuracy assessed, which satisfies the project objectives. A drawback of having a single face is that the accuracy and ease of being able to combine different DSM faces of the skull cannot be assessed.

In earlier attempts of creating a DSM, particularly at the USQ Laboratory, there were a large number of unwanted points or noise in the DSM. Manual deletion of the unwanted points is the only option to remove them and this took a significant amount of time, which is the reason further attempts of improving the DSM were pursued. The final DSM using the tinted skull photographed in natural light had minimal amounts of unwanted points.

The DSM and Points could be exported into a number of different file types, see Figure 3.7. The final DSM was exported to a DXF file type for use in AutoCAD. A number of options can be used to control what layers or objects are exported as part of the DXF file. In this case, the point mesh, DSM, targets and drawn lines (used for comparing measurements, discussed later) were exported successfully.

Using AutoCAD in 3D Modelling was tiresome due to the limitations of the computer used. The program was slow and became unresponsive a number of times, especially when zooming, rotating or moving the model or attempting to select large areas of points. The model window in PM proved easier and quicker to use for taking measurements and showing a photo-realistic DSM.

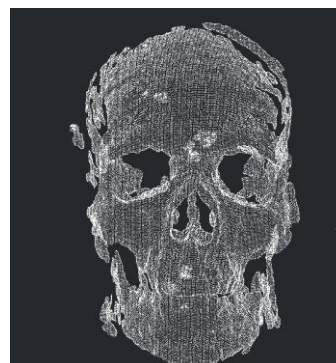
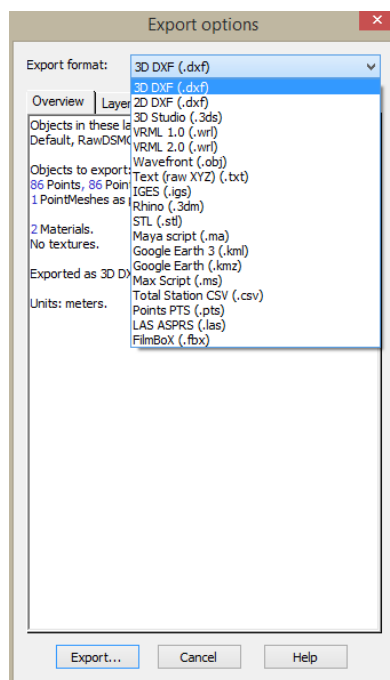


Figure 3.7 Export options (left) and screen shot of resulting DXF file in AutoCAD

3.9 Assessment of Accuracy

Both targets and points on the skull were used to assess the accuracy of the model. Points drawn on the skull prior to photo acquisition with pen were marked digitally in PM, using the *Mark Points Mode* in the *Marking* menu. (See Image 3.5 below) All photos in which a particular point can be seen is marked on each photo. After the points were marked, lines can be drawn between the points and the length of lines can be displayed using the *Measurements Pane*. (See Figure 3.8 below)

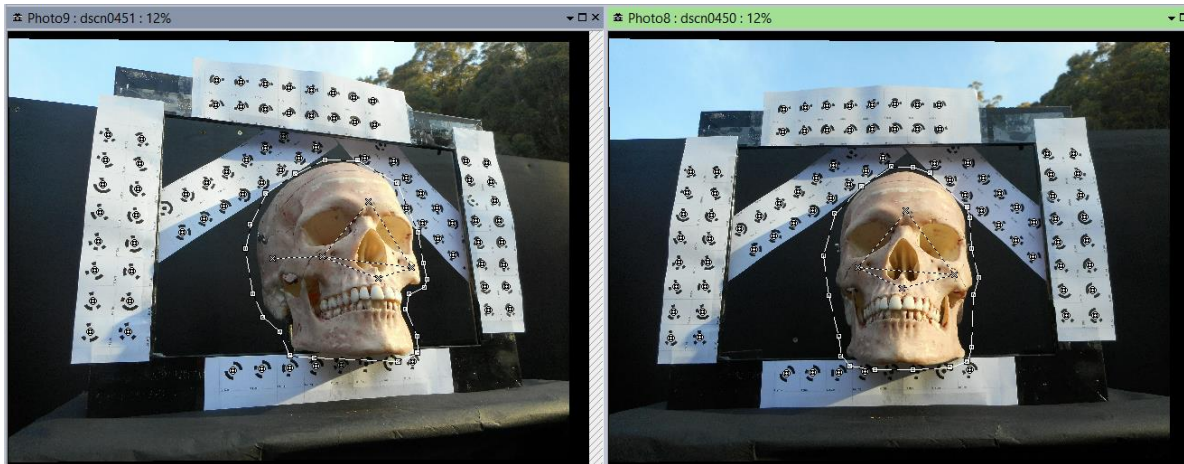


Image 3.5 Marking points on the skull for measurement.

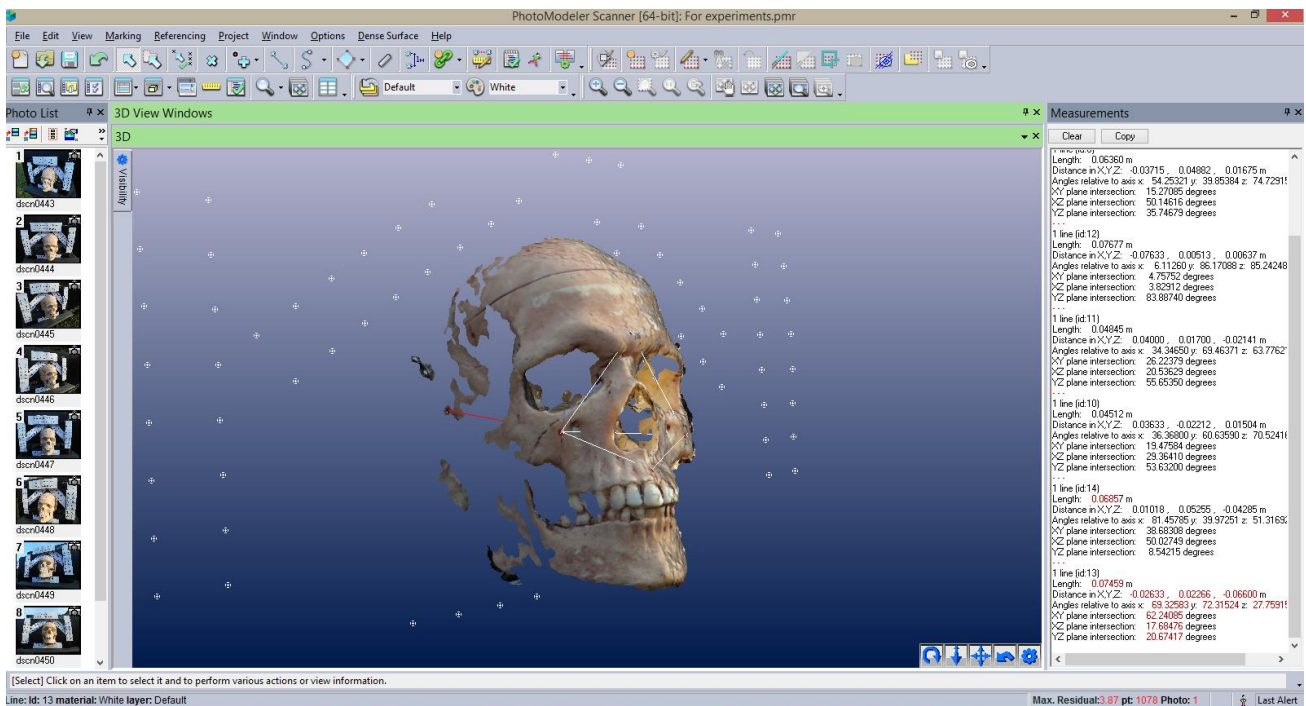


Figure 3.8 Screen shot of PM, note the Measurements pane on the right.

Measurements between the targets can also be displayed using this tool. (See Figure 3.9 below)

The measurements taken digitally can then be compared to measurements taken externally; callipers and measuring tape. Using the callipers and tape to measure between targets worked very well, as the targets are flat. Most of target to target measurements could not be measured using the callipers, as the length exceeded the range of the calliper; >200mm.

Measuring points on the skull was more difficult, especially using a tape measure. Using the tape to measure between points on flat parts of the skull was easier, however, estimating the measurement to a sub millimetre level is subject to observer error. Measurements of the skull points taken with the digital calliper are more useful than the tape, as the calliper can read to 0.01mm.

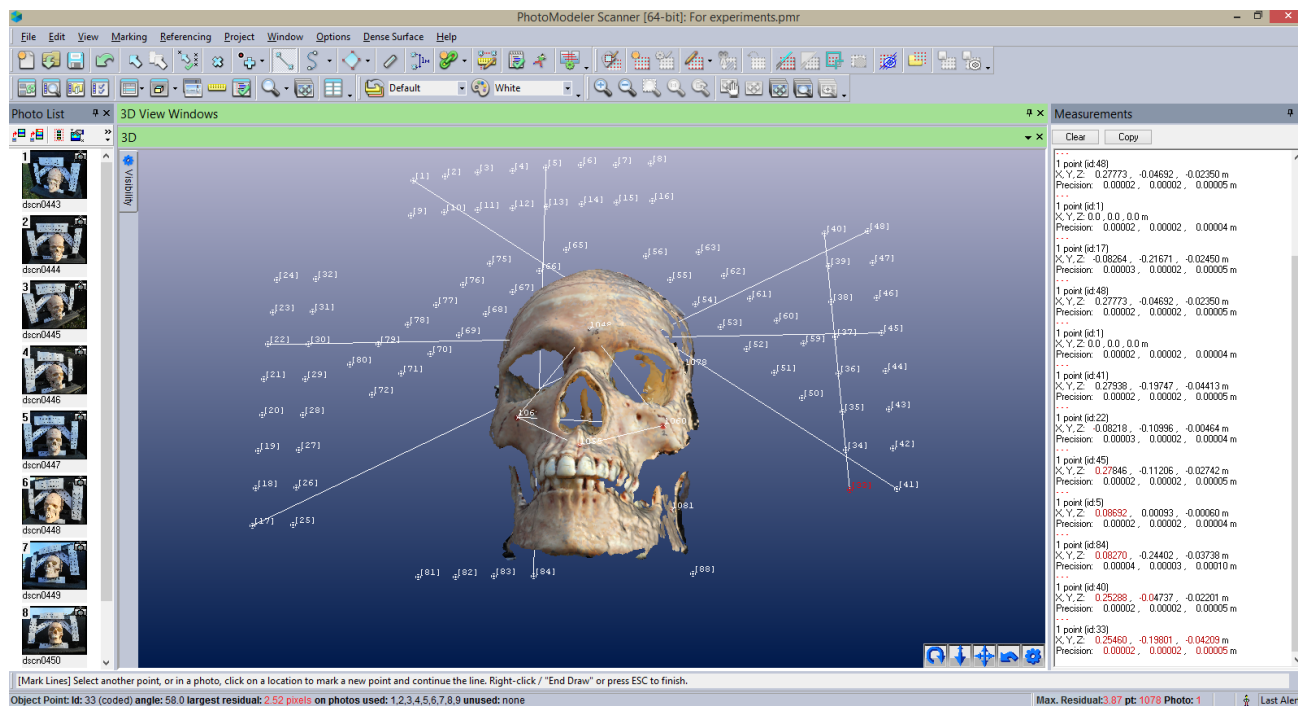


Figure 3.9 Screen shot showing measurements between selected targets.

4.0 Chapter Four – Results and Discussion

4.1 Camera Calibration

Three calibrations (3 sets per camera) were performed using three sets of data to attempt to improve the calibration results, see Table 4.1. However, the best calibration (lowest maximum residual) was the first calibration performed in the USQ Laboratory. (See Table 4.2 for full results)

Calibration ID	Comments
Red Set A Blue Set A	The first calibration sets attempted at the USQ Photogrammetry Lab
Red Set B Blue Set B	Calibration performed off campus. Camera settings adjusted and stronger lighting adopted.
Red Set C Blue Set C	Calibration performed off campus. Camera settings adjusted and calibration grid set up closer to camera to improve photograph coverage with lighting adjustments.

Table 4.1 Calibration sets completed and comments.

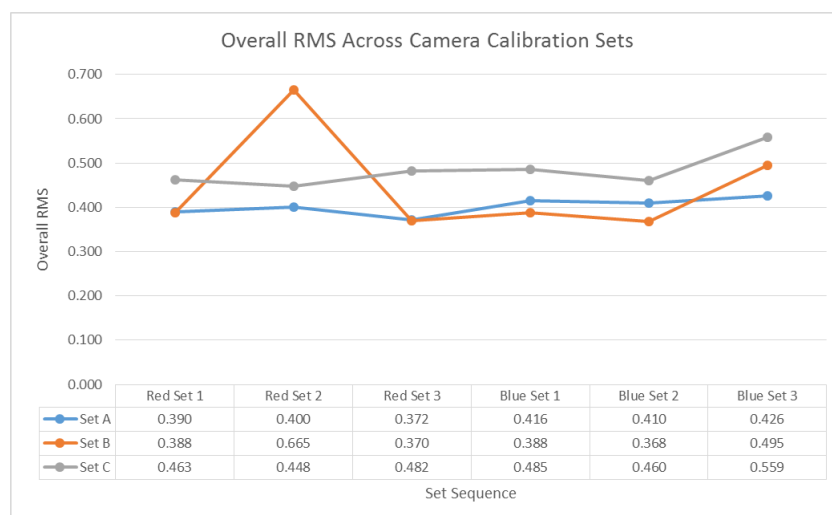


Figure 4.1 Overall RMS for all three sets.

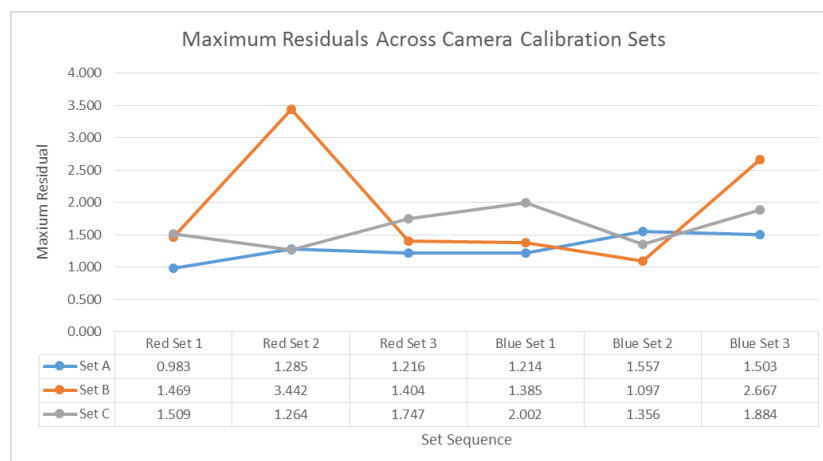


Figure 4.2 Maximum residuals for all three sets.

4.1.1 Results of Calibration

Calibration Set	Focal Lth	Xp	Yp	Fw	Fh	K1	K2	K3	P1	P2	Overall RMS	Max Residual
Red Set A 1	4.80835500	3.31388800	2.42188200	6.48033000	4.86000000	0.00026690	0.00001061	0.00000000	-0.00117800	-0.00004575	0.390	0.983
Red Set A 2	4.79843800	3.30672200	2.42120800	6.47820300	4.86000000	0.00043960	0.00000000	0.00000000	-0.00107500	-0.00010890	0.400	1.285
Red Set A 3	4.79071600	3.29069800	2.43371200	6.47953600	4.86000000	0.00039550	0.00003105	0.00000000	-0.00075840	0.00012950	0.372	1.216
Blue Set A 1	4.85448000	3.34207300	2.43645400	6.48285000	4.86000000	0.00042980	-0.00005714	0.00000000	-0.00176300	0.00023960	0.416	1.214
Blue Set A 2	4.84141000	3.32898600	2.44414600	6.48173800	4.86000000	0.00023880	0.00000000	0.00000000	-0.00148700	0.00034540	0.410	1.557
Blue Set A 3	4.83674000	3.32833500	2.44518900	6.48078700	4.86000000	0.00037640	-0.00001739	0.00000000	-0.00150000	0.00037090	0.426	1.503
Red Set B 1	4.81893200	3.31501300	2.42588600	6.48541100	4.86000000	0.00089370	-0.00015700	0.00000000	-0.00103700	0.00000000	0.388	1.469
Red Set B 2	4.81756900	3.30777800	2.42346700	6.47852700	4.86000000	0.00214700	-0.00054510	0.00000000	0.00101800	0.00000000	0.665	3.442
Red Set B 3	4.81632700	3.31104700	2.43134900	6.48164700	4.86000000	0.00124000	-0.00024660	0.00000000	-0.00102700	0.00015140	0.370	1.404
Blue Set B 1	4.86034500	3.35882700	2.44206100	6.48086600	4.86000000	0.00178300	-0.00053790	0.00000000	-0.00196700	0.00033560	0.388	1.385
Blue Set B 2	4.86173700	3.32426600	2.43927200	6.48128200	4.86000000	0.00176200	-0.00057590	0.00000000	-0.00127200	0.00037350	0.368	1.097
Blue Set B 3	4.85623800	3.33053400	2.44701800	6.48155100	4.86000000	0.00182500	-0.00045190	0.00000000	-0.00150300	0.00046130	0.495	2.667
Red Set C 1	4.80913500	3.31721700	2.40963900	6.47650500	4.86000000	0.00055980	-0.00001529	0.00000000	-0.00134100	-0.00025130	0.463	1.509
Red Set C 2	4.80136000	3.28493700	2.42092100	6.47442800	4.86000000	0.00053720	-0.00001928	0.00000000	-0.00073040	-0.00014080	0.448	1.264
Red Set C 3	4.80185100	3.30448100	2.41131200	6.47408900	4.86000000	0.00052650	-0.00001570	0.00000000	-0.00114100	-0.00032120	0.482	1.747
Blue Set C 1	4.83451900	3.32712600	2.43492100	6.47441700	4.86000000	0.00023230	-0.00002782	0.00000000	-0.00158400	0.00019410	0.485	2.002
Blue Set C 2	4.84708300	3.33801200	2.42047200	6.47564400	4.86000000	0.00025480	-0.00002184	0.00000000	-0.00180600	-0.00004686	0.460	1.356
Blue Set C 3	4.83597300	3.32679500	2.43544000	6.47601900	4.86000000	0.00022310	-0.00003413	0.00000000	-0.00160700	0.00020020	0.559	1.884

Table 4.2 Camera calibration results showing parameters, Root Mean Squared (RMS) and Maximum Residual

4.1.2 Discussion of Calibration Results

A number of difficulties were encountered during the calibration phase of the project, which is the reason a number of calibrations were performed to examine if the calibration results could be improved. The best result was the first calibration set (Red Set A 1), see Table 4.2 above, which was performed in the USQ Laboratory. As shown in Figure 4.1 and Figure 4.2, Red Set B 2 produced a spike in results, but Set A and C have closer similarity. The conditions in the laboratory differed to those off campus in the following ways:

Lighting

Lights (LED and halogen) were used off campus, which created some shadowing of the tripod and camera which was controlled where possible (e.g. placing the camera so that shadows did not fall across the calibration sheet). This could have created a poorer camera position geometry as the shadows were the concern, not the camera position. The lighting in the Laboratory was duller but did not cast shadows.

Percentage of calibration sheet in photo

The percentage of the calibration sheet in the photo was less in the off campus calibrations than on campus. The reason for this is that a larger tripod was used off campus; the smaller tripod on campus allowed the camera to be set up closer to the calibration sheet. A small table was used to attempt to improve the distance between the camera and calibration sheet, however, the tripod continued to cause problems due to the size. It also increased the risk of bumping the table causing the calibration sheet to move.

4.2 Photograph Capture and Processing

The final model was produced off campus after tinting the skull with acrylic paint. The following (Figure 4.3 and Figure 4.4) are images from PM of the 3D model represented in different ways:

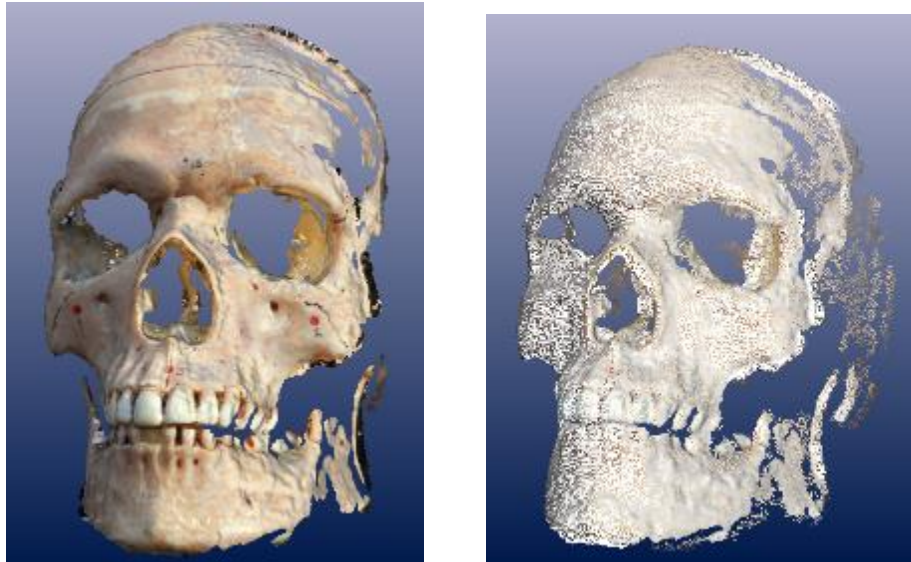


Figure 4.3 DSM coloured with photo texture (left) & DSM using single texture with points coloured with photo texture (right).

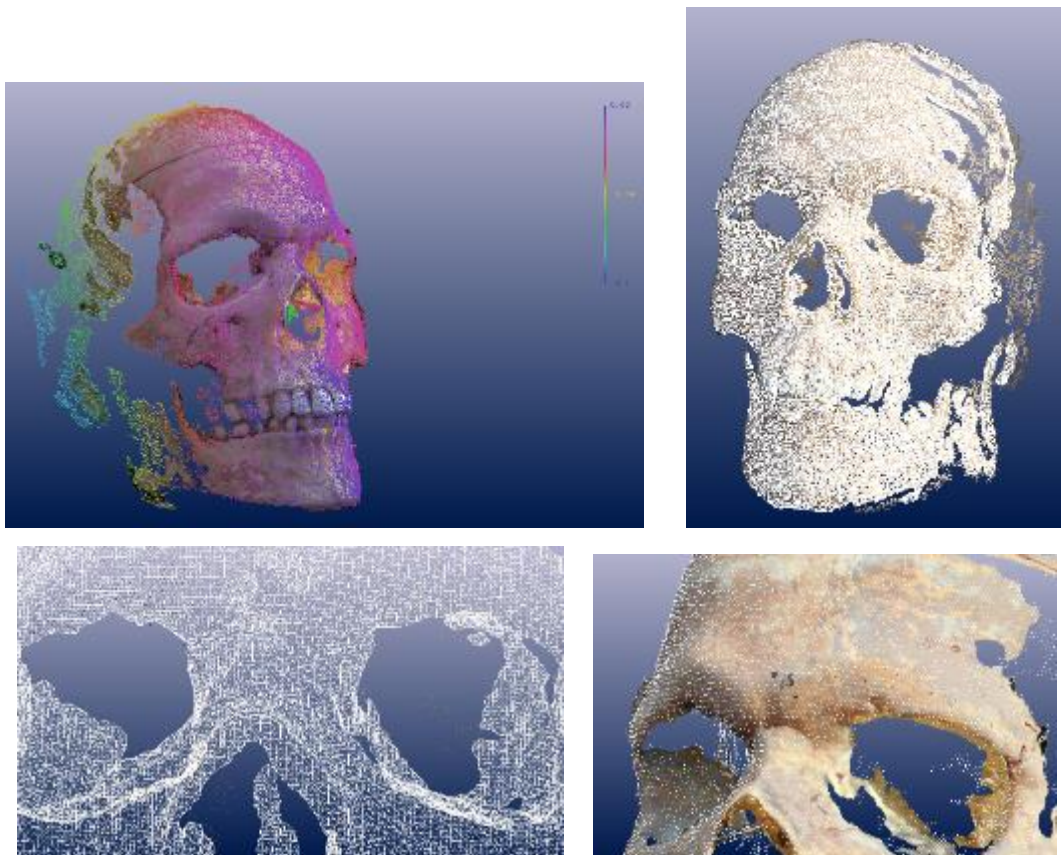


Figure 4.4 DSM with points coloured by depth (top left), DSM points coloured by photo texture overlaid with point cloud (top right), DSM shown as triangulated mesh (bottom left) and DSM showing close correlation with point cloud underneath (bottom right).

4.2.1 Discussion of Model Results

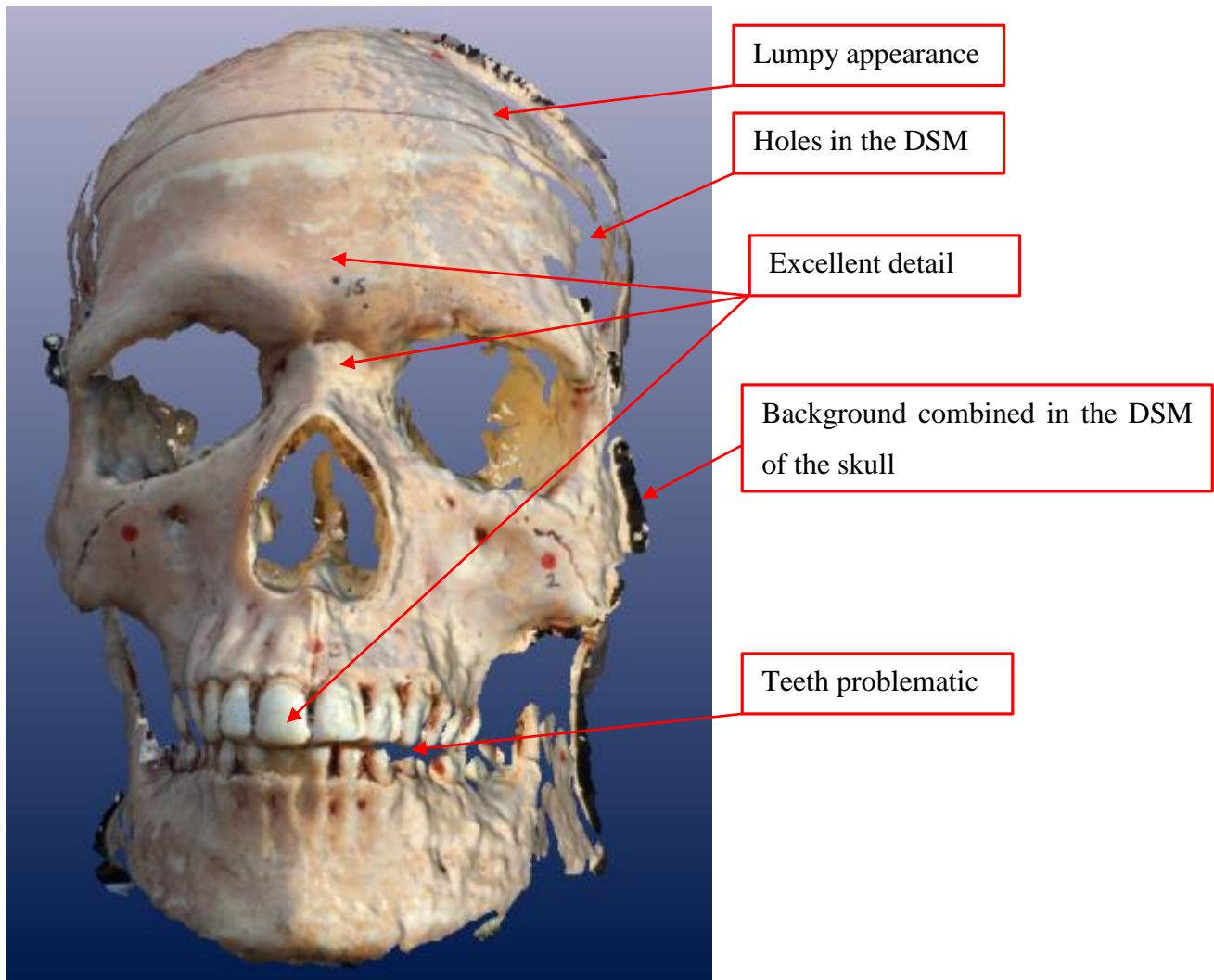


Figure 4.5 DSM with comments.

Figure 4.5 above shows the DSM with some comments on good and poor aspects of its appearance. There is some areas of lumpy appearance, which is an indicator of poor modelling. In earlier unsuccessful attempts of DSM creation the whole surface was lumpy. There are also some holes in the DSM which is a problem. These issues could perhaps be overcome if more sides of the skull were modelled and these sides combined to create a more complete model, as the camera angles could capture those areas which are lumpy and have holes. The teeth are also problematic, however, as mentioned in the literature, researchers have had problems modelling small details such as individual toes (Al-Baghdadi et al. 2011) or the sides of objects which are sitting against a surface, such as a table. (Urbanová, Hejna & Jurda 2015) This is perhaps a limitation of CRP which needs to be considered when one assesses the suitability of the technology for their application.

Some of the background has combined with the DSM, shown above (Figure 4.5). This could be trimmed away; the DSM shown has not been trimmed or modified, it is the direct result of the DSM

creation process. (See Appendix D) Despite these issues, there are areas of excellent detail. The processing and image acquisition are simple to perform; it is the awareness of all the separate issues which can affect the DSM which needs to be known and addressed if a 3D model is to be successful.

4.3 Measurements and Accuracy

The accuracy of the final model can be stated as being on average +/- 0.4mm across the project.

4.3.1 Skull Measurements

Measurement	Calliper	Tape	Model	Δ Model - Calliper	Δ Model-Tape
Point 1 – Point 2	76.64	-	76.77	0.13	
Point 1 – Point 3	44.48	44.5	45.12	0.64	0.6
Point 1 – Point 12	74.45	-	74.59	0.14	
Point 1 – Point 15	59.60	59.5	59.60	0.00	0.1
Point 2 – Point 3	47.43	48.0	48.45	1.02	0.4
Point 2 – Point 5	68.95	-	68.57	-0.38	
Point 2 – Point 15	63.34	63.5	63.60	0.26	0.1
Mean				0.26	0.30

Table 4.3 Measurements taken on skull (millimetres).

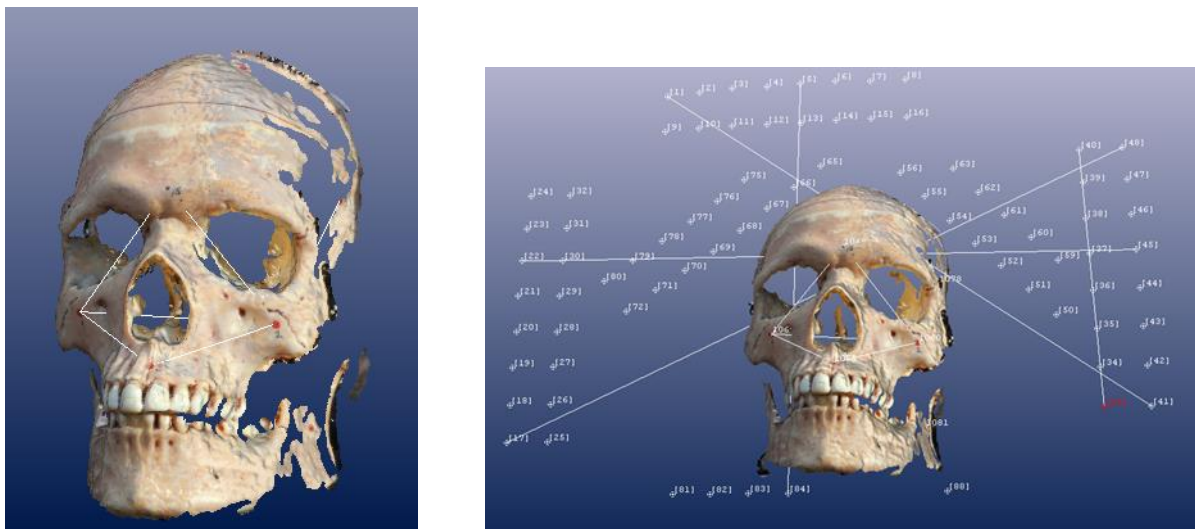


Figure 4.6 Skull showing measurements mentioned in Table 4.3 (left) & Table 4.4 (right).

4.3.2 Check on Accuracy

Measurement	Calliper	Tape	Model	Δ Model - Calliper	Δ Model-Tape
Target 17 – Target 48		397.5	398.37		0.87
Target 1 – Target 41		344.5	344.95		0.45
Target 22 – Target 45		362.0	361.36		-0.64
Target 5 – Target 84		247.0	247.74		0.74
Target 40 – Target 33	151.62	151.21	151.98	0.36	0.77
Mean				0.36	0.438

Table 4.4 Check measurements between targets (millimetres.)

4.3.3 Discussion of Results

The results of the accuracy of the model is acceptable and satisfactory for the project – overall a good result. The overall accuracy across the project is consistent with results mentioned in Table 2.1 of research papers which have used PM. The accuracy could certainly be improved by following the photo acquisition steps more rigorously – with careful attention to camera angles, lighting, target positioning and increasing the number of targets.

The assessment of accuracy could also be improved, by using a scale to estimate accuracy instead of a calliper and tape. As previously mentioned, the callipers were not large enough to measure between the targets and estimating sub-millimetre readings from the tape is open to observer error. To take accuracy estimation to a high level again, a control target coordinate network could be measured using survey equipment and the CRP results compared to these values.

Despite the improvements which can be made to both increasing the accuracy of the model and targets, and the methods used to estimate accuracy, the results attained are appropriate for this kind of project involving a skull. To be able to compare skulls or keep a record of a skull for forensic purposes – 0.4mm accuracy is sufficient.

4.3.4 Summary of Objectives Achieved

Objective 1: Camera Calibration - Determine the most appropriate calibration for the task, including the coded target type, number of targets and discuss any differences between the two cameras.

The most appropriate calibration for the task was the single sheet method, as recommended by Photomodeler, on an A3 sized piece of paper which covered the size of the skull. There were no significant differences between the two identical cameras; Red and Blue.

Objective 2: Image Acquisition - Determine the optimal amount of targets to be used and configuration.

The optimal target configuration was to use two rows of targets on the top, right and left side of the frame, as well as two rows diagonally, both top left and top right. One row of targets was also placed at the bottom as two rows would not fit. Targets could also be placed on the skull itself but that would add more time to the amount of processing to remove them from the model and it was found that tinting the skull helped to improve the DSM without adding targets to the skull itself.

Objective 3: Data Processing and Creation of 3D Model - Analyse the level of difficulty and note any problems in the creation of the 3D model from the images.

There were a number of difficulties experienced in the processing and creation of the 3D model, which some related to the photo acquisition. The target configuration, background, lighting, camera position and angle in relation to the skull, and skull material and texture all contributed to difficulties in processing, poor DSMs or inability to produce a DSM. After these issues were improved, further difficulties in the processing occurred, which included the depth at which the DSM processed the image and the method of using all photos to create the DSM. These two problems were overcome by setting a depth limit and choosing matching pairs to create the DSM.

The data processing and creation of a DSM are not difficult; it is the number of factors needed for consideration to achieve success which caused the problems. The image acquisition and processing issues can be overcome easily by following advice available in the literature and Photomodeler tutorials. Also putting time into experimenting with different techniques was useful to address problems unique to modelling the skull.

Objective 4: Accuracy of Results - Assess the accuracy of the 3D model comparing measurements taken with callipers and tape.

The accuracy of the 3D skull model assessed by comparing measurements of the model with those taken by a tape and callipers. The results are in close agreement, with the biggest residual being 1.02mm between two points on the skull. The average accuracy across the project was approximately 0.4mm. These results are satisfactory for the project and show that there are no gross errors or substantial inaccuracy.

5.0 Chapter Five - Conclusions

5.1 Introduction

There is much literature written on the benefits of using CRP for a number of applications, including human body mapping. While there is wide agreement that CRP is a useful tool which has advantages over other technologies there are also a number of issues which can occur in the process of creating a 3D model. CRP may not be suitable for some applications and to achieve success may take a number of trials, depending on the environment and conditions.

5.2 Conclusions

The number of variables and aspects to “get right” were underestimated initially; there are many opportunities for “things to go wrong” and affect the DSM creation in PM. Solving those problems took a significant amount of time, mainly through trial and error, which decreased the amount of time in the project time frame to be able to work on other tasks, such as creating a complete model. However, practise is a good way to learn about what kind of issues will affect a project, as using a different object may have raised different issues.

The difficulty in using a tape in particular to measure points on a curved object, such as the skull, was overlooked. A better method for comparing a highly accurate method of measurement like CRP would have been more appropriate, such as using a scale bar in the photos to estimate accuracy. The callipers worked well on the skull but were not long enough to measure between the targets on the control frame.

Photomodeler performed well and was relatively simple to learn to use the basics of the program. There was no prior knowledge of using Photomodeler and the tutorials provided with the product are very useful and assisted in learning. There are many more functions and useful tools in Photomodeler than are discussed in this project. More time dedicated to learning Photomodeler would have been better.

All things considered, the accuracy attained and methods used in this project are appropriate for modelling an object such as a skull. The project is useful for detailing and emphasising good practice and stressing that following steps thoroughly is important in producing successful, quality results. All of the project objectives were successfully completed:

Objective	Completed
<i>Objective 1:</i> Camera Calibration - Determine the most appropriate calibration for the task, including the coded target type, number of targets and discuss any differences between the two cameras.	✓
<i>Objective 2:</i> Image Acquisition - Determine the optimal amount of targets to be used and configuration.	✓
<i>Objective 3:</i> Data Processing and Creation of 3D Model - Analyse the level of difficulty and note any problems in the creation of the 3D model from the images.	✓
<i>Objective 4:</i> Accuracy of Results - Assess the accuracy of the 3D model comparing measurements taken with callipers and tape.	✓

5.3 Further Research and Recommendations

For students wishing to continue research on this topic, it is recommended to consider all the variables which can affect the quality and success of the model before capturing images. Much time has been dedicated to working through the issues, in which more time could have been dedicated to the development of the model if overcome earlier in the project time frame.

Exploring further use of Photomodeler and utilising other tools in the software is also an improvement which can be implemented. There is also the option of comparing Photomodeler's calibration process to that of other software, such as Australis, to examine any differences.

To take this project a step further, combining different faces or sides of the same model to create a complete 360° 3D model would be useful and interesting to examine. Using a scale bar to assess accuracy would also be another way to improve the analysis of accuracy for this kind of CRP project.

References

- Al-Baghdadi, JA, Chong, AK, McDougall, K & Alshadli, D 2012, 'An investigation of the 3-dimensional surface capture techniques of the human foot', in *International Workshop on Geoinformation Advances 2012: proceedings of the International Workshop on Geoinformation Advances 2012*, AA Rahman, et al. (eds.), Universiti Teknologi Malaysia, Johor Bahru, Malaysia, pp. 26-47, <<http://eprints.usq.edu.au/22494/>>.
- Al-Baghdadi, JAA, Chong, AK & Alshadli, D 2013, 'Compensation of measurement errors caused by glass refraction for photogrammetric plantar surface mapping', *Photogrammetric Record*, vol. 28, no. 143, pp. 261-75.
- Al-Baghdadi, JAA, Chong, AK, McDougall, K, Alshadli, D, Milburn, P & Newsham-West, R 2011, 'A dense surface modelling technique for foot surface imaging', in *2011 Surveying and Spatial Sciences Conference: Innovation in Action: Working Smarter (SSSC 2011): proceedings of the 2011 Surveying and Spatial Sciences Conference: Innovation in Action: Working Smarter (SSSC 2011)* Scion, Wellington, New Zealand, pp. 295-302, <<http://eprints.usq.edu.au/20586/>>.
- Alshadli, D, Chong, AK, Newsham-West, R, Al-Baghdadi, JAA, Milburn, P & McDougall, K 2013, 'A comparison between static and dynamic foot mobility magnitude measures', in *International Conference on Biomechanics in Sports: proceedings of the International Conference on Biomechanics in Sports*, H Toby (ed.), National Taiwan Normal University, Taipei, <<http://eprints.usq.edu.au/25083/>>.
- Alshadli, D, Chong, AK, McDougall, K, Al-Baghdadi, J, Milburn, P & Newsham-West, R 2013, 'Reliability of a high accuracy image-based system for 3D modelling of the medial longitudinal arch during gait', in *International Workshop on Geoinformation Advances 2012: proceedings of the International Workshop on Geoinformation Advances 2012*, AA Rahman, et al. (eds.), Springer-Verlag, Johor, Malaysia, pp. 85-101, <<http://eprints.usq.edu.au/23440/>>.
- Ayoub, AF, Xiao, Y, Khambay, B, Siebert, JP & Hadley, D 2007, 'Towards building a photo-realistic virtual human face for craniomaxillofacial diagnosis and treatment planning', *International Journal of Oral and Maxillofacial Surgery*, vol. 36, no. 5, pp. 423-8, Scopus.
- Cevidanes, LHC, Motta, A, Proffit, WR, Ackerman, JL & Styner, M 2010, 'Cranial base superimposition for 3-dimensional evaluation of soft-tissue changes', *American Journal of Orthodontics and Dentofacial Orthopedics*, vol. 137, no. 4 SUPPL., pp. S120-S9, Scopus.
- Chong, AK-F 2006, 'Photogrammetry for digital hand surface capture in swimming performance study', in *ISPRS Commission V Symposium: Image Engineering and Vision Metrology: proceedings of the ISPRS Commission V Symposium: Image Engineering and Vision Metrology*, HG Maas & D Schneider (eds.), International Society for Photogrammetry and Remote Sensing (ISPRS), Dresden, Germany, pp. 74-7, <<http://eprints.usq.edu.au/7371/>>.
- Chong, AK 2002, 'A Rigorous Technique for Forensic Measurement of Surveillance Video Footage', *Photogrammetric Engineering & Remote Sensing*, vol. 68, no. 7, pp. 753-9.
- Chong, AK 2011, 'Low-cost compact cameras: A medical application in CMT disease monitoring', *Photogrammetric Record*, vol. 26, no. 134, pp. 263-73, Scopus.

Chong, AK, Milburn, P, Newsham-West, R & ter Voert, M 2009, 'High-accuracy photogrammetric technique for human spine measurement', *Photogrammetric Record*, vol. 24, no. 127, pp. 264-79, Scopus.

Chong, AK, Majid, ZB, Ahmad, AB, Setan, HB & Samsudin, ABR 2004, 'The use of a national craniofacial database', *New Zealand Surveyor*, no. 294, pp. 15-8.

Dellepiane, M, Dell'Unto, N, Callieri, M, Lindgren, S & Scopigno, R 2013, 'Archeological excavation monitoring using dense stereo matching techniques', *Journal of Cultural Heritage*, vol. 14, no. 3, pp. 201-10, Scopus.

EoS Systems Inc. 2013, *User's Manual of PhotoModeler Scanner 2013*, EoS Systems Inc.,.

EoS Systems Inc. 2015, *Photomodeler*, EoS Systems Inc., <<http://www.photomodeler.com/index.html>>.

Fryer, J 2001, *Close range photogrammetry and machine vision*, [New ed.]. edn, Whittles, Caithness.

Fryer, J, Mitchell, H & Chandler, JH 2007, *Applications of 3D measurement from images*, Whittles, Dunbeath.

Low cost 3D face scanning based on landmarks and photogrammetry: A new tool for a surface diagnosis in orthodontics, Key Subjects <<http://www.scopus.com/inward/record.url?eid=2-s2.0-84867284478&partnerID=40&md5=163b2f4a867315ca394cde88cf8e27c3>>.

Galantucci, LM, Lavecchia, F, Percoco, G & Raspatelli, S 2014, 'New method to calibrate and validate a high-resolution 3D scanner, based on photogrammetry', *Precision Engineering*, vol. 38, no. 2, pp. 279-91, Scopus.

Green, J, Matthews, S & Turanli, T 2002, 'Underwater archaeological surveying using PhotoModeler, VirtualMapper: different applications for different problems', *The International Journal of Nautical Archaeology*, vol. 31, no. 2, pp. 283-92.

Guarnieri, A, Pirotti, F & Vettore, A 2010, 'Cultural heritage interactive 3D models on the web: An approach using open source and free software', *Journal of Cultural Heritage*, vol. 11, no. 3, pp. 350-3, Scopus.

Hassan, MFA, Ma'Arof, I & Samad, AM 2014, 'Assessment of camera calibration towards accuracy requirement', in *Proceedings - 2014 IEEE 10th International Colloquium on Signal Processing and Its Applications, CSPA 2014: proceedings of the Proceedings - 2014 IEEE 10th International Colloquium on Signal Processing and Its Applications, CSPA 2014* pp. 123-8, <<http://www.scopus.com/inward/record.url?eid=2-s2.0-84901685922&partnerID=40&md5=b9e47f1fe42d02f6431a2a6b3ba8848e>>.

Hernán-Pérez, AS, Domínguez, MG, González, CR & Martín, AP 2013, 'Using iphone camera in photomodeler for the 3D survey of a sculpture as practice for architected students', in *Procedia Computer Science: proceedings of the Procedia Computer Science* pp. 345-7, <<http://www.scopus.com/inward/record.url?eid=2-s2.0-84890773624&partnerID=40&md5=14faa6e06c5fb4c8a8de98d58c62a1c2>>.

Hoevenaren, IA, Maal, TJJ, Krikken, E, De Haan, AFJ, Bergé, SJ & Ulrich, DJO 2015, 'Development of a three-dimensional hand model using 3D stereophotogrammetry: Evaluation of landmark reproducibility', *Journal of Plastic, Reconstructive and Aesthetic Surgery*, vol. 68, no. 5, pp. 709-16, Scopus.

Hoogeboom, B, Alberink, I & Goos, M 2009, 'Body height measurements in images', *Journal of Forensic Sciences*, vol. 54, no. 6, pp. 1365-75, Scopus.

Katz, D & Friess, M 2014, 'Technical Note: 3D From Standard Digital Photography of Human Crania—A Preliminary Assessment', *American Journal of Physical Anthropology*, vol. 154, no. 1, pp. 152-8.

Krajňák, M, Pukanská, K & Bartoš, K 2011, 'Application of digital photogrammetry in the process of documentation of archaeological artefacts', *Acta Montanistica Slovaca*, vol. 16, no. 4, pp. 337-43, Scopus.

Luhmann, T, Robson, S, Kyle, S & Harley, I 2006, *Close range photogrammetry : principles, techniques and applications*, Whittles Publishing, Caithness Scotland.

Lynnerup, N, Andersen, M & Lauritsen, HP 2003, 'Facial image identification using Photomodeler®', *Legal Medicine*, vol. 5, no. 3, pp. 156-60, Scopus.

Majid, Z, Chong, AK, Ahmad, A, Setan, H & Samsudin, AR 2005, 'Photogrammetry and 3D laser scanning as spatial data capture techniques for a national craniofacial database', *Photogrammetric Record*, vol. 20, no. 109, pp. 48-68.

Majid, ZC, A. K.; Setan, H.; Ahmad, A.; Rani Samsudin, A.; 2005, 'Photogrammetry and 3D Laser Scanning as Spatial Data Capture Techniques for a National Craniofacial Database', *The Photogrammetric Record*, vol. 109, no. 20, pp. 48-68.

Oniga, VE & Chirilă, C 2013, 'Object Based Digital Non-Metric Images Accuracy ', *13th SGEM GeoConference on Informatics, Geoinformatics And Remote Sensing*, vol. 2, no. June 16-22, pp. 655-62.

Percoco, G, Galantucci, LM & Lavecchia, F 2011, '3D digitization of curves on human bodies by means of digital close range photogrammetry', in *Annals of DAAAM and Proceedings of the International DAAAM Symposium: proceedings of the Annals of DAAAM and Proceedings of the International DAAAM Symposium* pp. 1371-2, <<http://www.scopus.com/inward/record.url?eid=2-s2.0-84904289537&partnerID=40&md5=d2edd3449d33622adfcda17ab16cde3b>>.

Rahman, SA & Alam, MK 2013, 'Validity of close range photogrammetry technique on craniofacial soft tissue measurement', *International Medical Journal*, vol. 20, no. 5, pp. 601-4, Scopus.

Randles, B, Jones, B, Welcher, J, Szabo, T, Elliott, D & MacAdams, C 2010, 'The accuracy of photogrammetry vs. hands-on measurement techniques used in accident reconstruction', *SAE Technical Papers*, Scopus.

Samper, D, Santolaria, J, Brosed, FJ, Majarena, AC & Aguilar, JJ 2013, 'Analysis of Tsai calibration method using two- and three-dimensional calibration objects', *Machine Vision and Applications*, vol. 24, no. 1, pp. 117-31, Scopus.

Sanz, JO, Docampo, MDLLG, Rodríguez, SM, Sanmartín, MTR & Cameselle, GM 2010, 'A simple methodology for recording petroglyphs using low-cost digital image correlation photogrammetry and consumer-grade digital cameras', *Journal of Archaeological Science*, vol. 37, no. 12, pp. 3158-69, Scopus.

Shigeta, Y, Hirabayashi, R, Ikawa, T, Kihara, T, Ando, E, Hirai, S, Fukushima, S & Ogawa, T 2013, 'Application of photogrammetry for analysis of occlusal contacts', *Journal of Prosthodontic Research*, vol. 57, no. 2, pp. 122-8, Scopus.

Slot, L, Larsen, PK & Lynnerup, N 2014, 'Photogrammetric Documentation of Regions of Interest at Autopsy- A Pilot Study', *Journal of Forensic Sciences*, vol. 59, no. 1, pp. 226-30, Scopus.

Udin, WS & Ahmad, A 2011, 'Calibration of high resolution digital camera using self-calibration bundle adjustment method', in Proceedings - 2011 IEEE 7th International Colloquium on Signal Processing and Its Applications, CSPA 2011: *proceedings of the Proceedings - 2011 IEEE 7th International Colloquium on Signal Processing and Its Applications, CSPA 2011* pp. 137-41, <<http://www.scopus.com/inward/record.url?eid=2-s2.0-79957480727&partnerID=40&md5=db2a07d9faef5077d373272dbe7ef4b8>>.

Urbanová, P, Hejna, P & Jurda, M 2015, 'Testing photogrammetry-based techniques for three-dimensional surface documentation in forensic pathology', *Forensic Science International*, vol. 250, pp. 77-86, Scopus.


Appendix A: Project Specification

ENG4111/4112 Research Project

STUDENT:	Heidi Belbin
TOPIC:	The use of low-cost photogrammetry techniques to create an accurate model of a human skull.
Supervisor:	Dr. Albert Kon-Fook Chong
Enrolment:	Research Project ENG4111 Semester 1, 2015 Research Project ENG4112 Semester 2, 2015
Project Aim:	Analyse the accuracy of using low-cost photogrammetry techniques to create a digital 3D model of a skull. Low-cost photogrammetry involves the use of low-cost, off the shelf cameras and low-cost software. (Photomodeler) A camera calibration will then be performed in a laboratory setting. Measurements taken from the digital model will be compared to traditional forms of measurement, such as with a tape and callipers.

Programme:

1. Research literature related to the following (To be well-covered before **MAY** 2015):
 - a. Previous studies involving close-range photogrammetry to create accurate 3D dense-surface models (particularly skulls and other complex shapes)
 - b. Digital camera calibration,
 - c. 3D dense surface capture software: Photomodeler software,
 - d. Techniques for measuring skulls with a tape and callipers,
 - e. Methods for calibrating tapes and callipers,
 - f. The benefits of using photogrammetry for applications in biological anthropology, archaeology, forensic investigation, medical applications and so on.
2. Select camera self-calibration technique and carry out the calibration and data acquisition at the Surveying Laboratory at USQ, Toowoomba in **MAY** 2015. This step also requires the following:
 - a. Purchase of two low-cost cameras (before arrival at lab)
 - b. The construction of a calibration grid and camera mount (will be carried out in the lab under supervision)
 - c. Borrow/purchase a high-quality human skull model (preferably a cast of a real skull)
3. Record measurements of the skull using traditional methods
4. Record measurements of 3D dense-surface model using Photomodeler and compare results with traditional measurements.

AGREED:	Heidi Belbin (Student)	 (Supervisor)
	Date: 12/03/2015	Date: 09/03/2015
	Examiner/Co-examiner: _____ Date:	

Appendix B: Photomodeler Referenced Material

The following are particular articles from EoS Systems Inc. (2015) which are useful for learning to use Photomodeler for 3D modelling:

1. Real world objects and materials that will and won't work well with PhotoModeler Scanner's DSM tools.

[<http://info.photomodeler.com/blog/kb/real_world_objects_and_materials_that_wi/>](http://info.photomodeler.com/blog/kb/real_world_objects_and_materials_that_wi/)

2. Improving Your Photo-Textures

[<http://info.photomodeler.com/blog/kb/improving_your_photo-textures/>](http://info.photomodeler.com/blog/kb/improving_your_photo-textures/)

3. Tips for improving PointMesh results in PhotoModeler Scanner

[<http://info.photomodeler.com/blog/kb/tips_for_improving_pointmesh_results_in_/>](http://info.photomodeler.com/blog/kb/tips_for_improving_pointmesh_results_in_/)

4. Animal Skull Scan

[<http://www.photomodeler.com/applications/biology/default.html>](http://www.photomodeler.com/applications/biology/default.html)

5. What is Camera Focal Length?

[<http://info.photomodeler.com/blog/kb/what_is_camera_focal_length/>](http://info.photomodeler.com/blog/kb/what_is_camera_focal_length/)

6. How accurate is PhotoModeler?

[<http://info.photomodeler.com/blog/kb/how_accurate_is_photomodeler/>](http://info.photomodeler.com/blog/kb/how_accurate_is_photomodeler/)

7. Glossary

[<http://www.photomodeler.com/support/glossary.html#F>](http://www.photomodeler.com/support/glossary.html#F)

Appendix C: Processing Report

Status Report Tree

Project Name: *** Project has not yet been saved ***

Problems and Suggestions (1)

Project Problems (1)

Problem: A large percentage of your points are sub-pixel marked so it is assumed you are striving for a high accuracy result. The largest residual (Point81 - 2.87) is greater than 1.00 pixels.

Suggestion: In high accuracy projects, strive to get all point residuals under 1.00 pixels. If you have just a few high residual points, study them on each photo to ensure they are marked and referenced correctly. If many of your points have high residuals then make sure the camera stations are solving correctly. Ensure that you are using the best calibrated camera possible. Remove points that have been manually marked unless you need them.

Problems related to most recent processing (0)

Information from most recent processing

Last Processing Attempt: Sun Oct 18 13:19:25 2015

Version: PhotoModeler Scanner 2015.1.1.1546 (64-bit)

Status: successful

Processing Options

Orientation: on

Only unoriented photos oriented.

Number of photos oriented: 9

Global Optimization: on

Calibration: off

Constraints: on

Total Error

Number of Processing Iterations: 8

Number of Processing Stages: 2

First Error: 4.075

Last Error: 6.537

Precisions / Standard Deviations

Photograph Standard Deviations

Photo 1: dscn0443.jpg

Omega

Value: -37.743287 deg

Deviation: Omega: 0.014 deg

Phi

Value: 22.508878 deg

Deviation: Phi: 0.010 deg

Correlations over 95.0%: X:98.2%

Kappa

Value: 9.393703 deg

Deviation: Kappa: 0.004 deg

Xc

Value: 0.652470

Deviation: X: 2.5e-004

Correlations over 95.0%: Phi:98.2%

Yc

Value: 1.009211

Deviation: Y: 3.2e-004

Zc

Value: -0.432959

Deviation: Z: 2.5e-004

Photo 2: dscn0444.jpg

Omega

Value: -34.843515 deg

Deviation: Omega: 0.015 deg

Correlations over 95.0%: Y:-98.8%, Z:97.2%

Phi

Value: -1.835337 deg

Deviation: Phi: 0.009 deg

Correlations over 95.0%: X:99.4%

Kappa

Value: -0.562110 deg

Deviation: Kappa: 0.003 deg

Xc

Value: -0.088793

Deviation: X: 2.7e-004

Correlations over 95.0%: Phi:99.4%

Yc

Value: 0.999216

Deviation: Y: 3.0e-004

Correlations over 95.0%: Omega:-98.8%

Zc
Value: -0.404634
Deviation: Z: 2.8e-004
Correlations over 95.0%: Omega:97.2%

Photo 3: dscn0445.jpg
Omega
Value: -40.977147 deg
Deviation: Omega: 0.014 deg

Phi
Value: -24.539233 deg
Deviation: Phi: 0.008 deg
Correlations over 95.0%: X:98.0%

Kappa
Value: -12.339340 deg
Deviation: Kappa: 0.004 deg

Xc
Value: -0.688116
Deviation: X: 2.0e-004
Correlations over 95.0%: Phi:98.0%

Yc
Value: 0.944714
Deviation: Y: 2.8e-004

Zc
Value: -0.494142
Deviation: Z: 2.5e-004

Photo 4: dscn0446.jpg
Omega
Value: -20.249879 deg
Deviation: Omega: 0.017 deg
Correlations over 95.0%: Y:-98.5%

Phi
Value: -27.491201 deg
Deviation: Phi: 0.010 deg
Correlations over 95.0%: X:98.6%

Kappa
Value: -3.410352 deg
Deviation: Kappa: 0.004 deg

Xc
Value: -0.727358
Deviation: X: 2.3e-004
Correlations over 95.0%: Phi:98.6%

Yc
Value: 0.596740
Deviation: Y: 4.0e-004
Correlations over 95.0%: Omega:-98.5%

Zc
Value: -0.313757
Deviation: Z: 2.1e-004

Photo 5: dscn0447.jpg
Omega
Value: -21.843332 deg
Deviation: Omega: 0.018 deg
Correlations over 95.0%: Y:-99.7%

Phi
Value: -3.845427 deg
Deviation: Phi: 0.011 deg
Correlations over 95.0%: X:99.6%

Kappa
Value: -0.159501 deg
Deviation: Kappa: 0.003 deg

Xc
Value: -0.053374
Deviation: X: 3.2e-004
Correlations over 95.0%: Phi:99.6%

Yc
Value: 0.637362
Deviation: Y: 4.2e-004
Correlations over 95.0%: Omega:-99.7%

Zc
Value: -0.243762
Deviation: Z: 2.0e-004

Photo 6: dscn0448.jpg
Omega
Value: -23.214555 deg
Deviation: Omega: 0.013 deg
Correlations over 95.0%: Y:-97.7%

Phi

Value: 19.695557 deg
 Deviation: Phi: 0.010 deg
 Correlations over 95.0%: X:98.8%
 Kappa
 Value: 3.210382 deg
 Deviation: Kappa: 0.003 deg
 Xc
 Value: 0.527951
 Deviation: X: 2.2e-004
 Correlations over 95.0%: Phi:98.8%
 Yc
 Value: 0.590299
 Deviation: Y: 2.9e-004
 Correlations over 95.0%: Omega:-97.7%
 Zc
 Value: -0.462130
 Deviation: Z: 1.6e-004
 Photo 7: dscn0449.jpg
 Omega
 Value: -0.537288 deg
 Deviation: Omega: 0.012 deg
 Correlations over 95.0%: Y:-99.4%
 Phi
 Value: 19.832007 deg
 Deviation: Phi: 0.012 deg
 Correlations over 95.0%: X:99.1%
 Kappa
 Value: -4.632261 deg
 Deviation: Kappa: 0.003 deg
 Xc
 Value: 0.599924
 Deviation: X: 3.1e-004
 Correlations over 95.0%: Phi:99.1%
 Yc
 Value: -0.032722
 Deviation: Y: 3.0e-004
 Correlations over 95.0%: Omega:-99.4%
 Zc
 Value: -0.179254
 Deviation: Z: 2.6e-004
 Photo 8: dscn0450.jpg
 Omega
 Value: -0.018633 deg
 Deviation: Omega: 0.015 deg
 Correlations over 95.0%: Y:-99.7%
 Phi
 Value: -0.036193 deg
 Deviation: Phi: 0.015 deg
 Correlations over 95.0%: X:99.8%
 Kappa
 Value: -0.000490 deg
 Deviation: Kappa: 0.003 deg
 Xc
 Value: -0.001104
 Deviation: X: 4.6e-004
 Correlations over 95.0%: Phi:99.8%
 Yc
 Value: 0.000555
 Deviation: Y: 4.4e-004
 Correlations over 95.0%: Omega:-99.7%
 Zc
 Value: 0.000097
 Deviation: Z: 9.3e-005
 Photo 9: dscn0451.jpg
 Omega
 Value: 0.803157 deg
 Deviation: Omega: 0.014 deg
 Correlations over 95.0%: Y:-99.6%
 Phi
 Value: -16.310541 deg
 Deviation: Phi: 0.012 deg
 Correlations over 95.0%: X:99.4%
 Kappa
 Value: 3.004587 deg
 Deviation: Kappa: 0.003 deg
 Xc
 Value: -0.572961

Deviation: X: 3.1e-004
 Correlations over 95.0%: Phi:99.4%
 Yc
 Value: -0.058564
 Deviation: Y: 3.6e-004
 Correlations over 95.0%: Omega:-99.6%
 Zc
 Value: -0.135599
 Deviation: Z: 2.1e-004

Quality

Photographs

- Total Number: 9
- Bad Photos: 0
- Weak Photos: 0
- OK Photos: 9
- Number Oriented: 9
- Number with inverse camera flags set: 0

Cameras

- Camera1: RED S1 COOLPIX S3700 [4.50]
- Calibration: yes
- Number of photos using camera: 9
- Average Photo Point Coverage: 50%

Photo Coverage

Referenced points outside of the camera's calibrated coverage region:

- Photo1 points outside region:#24, #48, #23, #22, #47, #21, #20
- Photo2 points outside region: more than 10 (check photo and calibration point coverage)
- Photo3 points outside region: more than 10 (check photo and calibration point coverage)
- Photo4 points outside region: more than 10 (check photo and calibration point coverage)
- Photo5 points outside region: more than 10 (check photo and calibration point coverage)
- Photo6 points outside region: more than 10 (check photo and calibration point coverage)
- Photo7 points outside region: more than 10 (check photo and calibration point coverage)
- Photo8 points outside region: more than 10 (check photo and calibration point coverage)
- Photo9 points outside region: more than 10 (check photo and calibration point coverage)

Point Marking Residuals

- Overall RMS: 0.819 pixels
- Maximum: 2.870 pixels
- Point 81 on Photo 4
- Minimum: 0.454 pixels
- Point 55 on Photo 4
- Maximum RMS: 1.667 pixels
- Point 81
- Minimum RMS: 0.324 pixels
- Point 68

Point Tightness

- Maximum: 0.0017 m
- Point 81
- Minimum: 0.00026 m
- Point 68

Point Precisions

- Overall RMS Vector Length: 0.000245 m
- Maximum Vector Length: 0.000464 m
- Point 84
- Minimum Vector Length: 0.000214 m
- Point 3
- Maximum X: 0.000209 m
- Maximum Y: 0.000172 m
- Maximum Z: 0.0004 m
- Minimum X: 8.81e-005 m
- Minimum Y: 7.8e-005 m
- Minimum Z: 0.000169 m

Point Angles

- Maximum: 64.02 degrees
- Point 14
- Minimum: 41.2 degrees
- Point 80
- Average: 58.56 degrees

Appendix D: Creating a 3D Dense Surface

The following is a step by step process of how a DSM was created for this project. Tutorial 2, Chapter 5 of the Photomodeler User's Manual 2013 details these steps to create a DSM of a foot print.

Getting Started

1. Open **Photomodeler** and start a new project, *Automated Targets*, for the *Getting Started* dialog.
2. Follow the *New Project Wizard* steps.
3. Select RAD – Coded Target Auto-project
4. Select photos of object to be modelled and press *Next*.
5. Select the camera from the *Library* you wish to use, e.g. **RED S1 COOLPIX S3700 [4.50]**
6. A dialog will appear, *Automated Coded Target Project*, select *Run...* When the process finishes, select *Close*.

Automated Target Marking

7. Go to the *Marking* menu, select *Automatic Target Marking...*
8. A dialog will appear, *Automatic Target Marking*, make sure *All Photos* is selected from the *Photos from set* option, and the correct *Target type* is selected, e.g. **12-Bit Coded**
9. Select *Mark Points*, wait for the process to finish and then select *Close*.
10. At this point, *Save* the project.

Process Project

11. Go to the *Project* menu and select *Process...*
12. A dialog will appear, *Processing*, accept default values and select *Process*
13. When the processing is complete, select **OK**. A report can also be saved to a text file to examine the quality of the project.
14. Go to the *Project* menu and select *Idealise Project*. A dialogue will appear stating this step is no longer necessary. Select either *Yes, show me the Idealize dialog* or *No, exit Idealize*. The tutorial suggestion was adopted to proceed to idealise the photos.
15. After the *Idealize* step has been completed, follow the prompts to *re-process* the project.

Create DSM

16. For each photo, create a trim around the object, in this case the skull. This can be done by selecting from the *Dense Surface* menu – *DSM Trim Mode*. Draw a line around the skull and double-click on the start of the line to end.

17. Go to the *Dense Surface* menu and select *Create Dense Surface*. In the *DSM Options* tab, select *Paired photos* to use for the DSM. Go through the list and tick the pairs to be used. In the *Settings* options, untick *Auto depth range* and enter an appropriate depth value for the project. In this case, 700mm was more than sufficient to capture the entire skull. Check the correct *Units* value as well to avoid errors.

18. Still in the *Create Dense Surface* window, go to the *Meshing Options* tab and select *Set Defaults*. Then *Execute*.

Scale Rotate Translate Project

19. Next a scale, coordinate system and rotation can be set for the project. In order to complete this, there must be a known measurement, such as between two targets, in the project. In the Project menu, there is an option to use the *Scale/Rotate Wizard* or *Scale/Rotate Viewer*. Either can be selected to set the parameters. For this project, the step by step wizard was initially followed and the *Scale/Rotate Viewer* was then used to make any changes necessary. The coordinate system used was simply to set a particular target as having coordinates, in this case, Point 1 was given X,Y,Z coordinates of 0.0, 0.0, and 0.0.

3D Model DSM

19. Open the *3D View Window* in the *Tools Bar*. There are a number of different surfaces that can be displayed and also measurements can be take using the *Measurements* tool between points and lines. The model can be exported to other file formats if required. There are many useful tools and display options available in the *3D View Window*.